Supporting Information

Heteroatoms-facilitated blue to near-infrared emission of nonconjugated polyesters

Xiong Liu[#], Bo Chu[#], Zuping Xiong, Bin Liu, Weihao Tu, Haoke Zhang*, Jing Zhi Sun*, Xinghong Zhang*, and Ben Zhong Tang*

Table of Contents

Materials

All manipulations involving air- and/or water-sensitive compounds were carried out with the standard Schlenk and vacuum line techniques under a nitrogen atmosphere or in a nitrogen-filled glovebox. Glutaric anhydride (GA), Diglycolic anhydride (DGA), (N-methylimino) diacetic acid anhydride (NDA), Thiodiglycolic anhydride (TDGA), propylene epoxide (PO), were purchased from Aldrich. Dimethyl Glutarate (M1), Dimethyl 2,2'-thiobisacetate (M4) were purchased from Macklin. Chromatographic purity solvents including toluene, dichloromethane, tetrahydrofuran (THF), n-Hexane, acetone, chloroform ($CHCl_3$), Dimethyl sulfoxide (DMSO), N, N-Dimethylformamide (DMF), Acetonitrile (ACN), ethanol, triethylamine (TEA), and flaky sodium hydroxide (CaH_2) were bought from SINOPHARM. Triethylborane (TEB, 1 M in THF) and Propylene sulfide (PS) were purchased from TCI. PO, TEA, M1, M4, and toluene were refluxed over CaH_2 for 24 h and vacuum-distilled prior to use. All the anhydrides were purified by vacuum sublimation two times. The purified anhydrides were collected under an inert atmosphere and stored in the glove box for use. Other organic reagents were used without purification.

Measurement

The polyester samples were characterized by nuclear magnetic resonance (^{1}H NMR and ^{13}C NMR), , gel permeation chromatography (GPC), fluorescence spectrophotometer, UV-vis spectrophotometer. NMR spectra were recorded on a Bruker 400 MHz instrument in $CDCl_3$ or $(CD_3)_2SO$ by using tetramethylsilane (TMS) as an internal reference. The number-averaged molecular weight (M_n) and polydispersity index (PDI) were obtained using a PL-GPC 220 chromatograph (Polymer Laboratories, Ltd., Santa Clara/United States) equipped with an HP 1100 pump from Agilent Technologies (Shanghai, China) and differential refractive index (dRI) detectors. The columns (4 x PLgel 5 µm MIXED-C, 300 x 7.5 mm) were eluted using chromatographic purity THF and DMF with 1.0 mL/min at 40 °C. The standards were monodisperse polystyrene covering the molecular weight from 200 to 2,000,000 Da. The standards were monodisperse polystyrene covering the molecular weight from 1000 to 10,000,000 Da. The copolymerized structures were characterized by matrix-assisted laser desorption ionization-time of flight mass spectrometry (MALDI-TOF MS) from Bruker ultra-extreme. Sodium trifluoroacetate was used as the cationization agent and trans-2-[3-(4-tert-Butylphenyl)-2-methyl-2-propenylidene] malononitrile (DCTB) was used as the matrix. Electron paramagnetic resonance (EPR) spectrum was recorded on an EPR-l: Bruker A300-band EPR. Photoluminescence spectra were collected from an FLS920 transient fluorescence spectrometer with an excitation source of a xenon lamp. Absolute quantum yields were obtained by additional integrating sphere. The fluorescence decay curves were recorded on an Instruments C11367 transient spectrometer. UV-Vis absorption spectra were recorded on the UV-vis spectrophotometer of Cary 100. The Photos were recorded by a Cannon EOS 90D.

Representative copolymerization procedures

Synthesis of P1~P4 catalyzed by TEA/TEB.

In a glovebox, TEA (2.8 µl, 20 µmol), TEB (20 µl, 20 µmol), PO (0.84 mL, 12.0 mmol) were measured into four 35.0 mL vials equipped with Teflon-coated stir bars. GA (456 mg, 4.0 mmol), DGA (464 mg, 4.0 mmol), NDA (516 mg, 4.0 mmol), TDGA (528 mg, 4.0 mmol) were added via syringes, respectively. The four vials were sealed with a Teflon-lined cap, removed from the glovebox, and immersed into an oil-bath preheated to 60 ℃. After 72 h reaction, the solution became viscous and transparent. The four vials were then removed from the heat block and cooled to room temperature. The mixtures of the four vials were dissolved in 1.5 mL DCM and then put into ca. 50 mL analytical ethanol (without PL response) to precipitate the products, respectively. The dissolve-precipitation process was repeated three times to remove unreacted monomers and catalysts. The polymers of **P1~P4** were finally collected and dried in vacuum at 45 ℃ for 12 h.

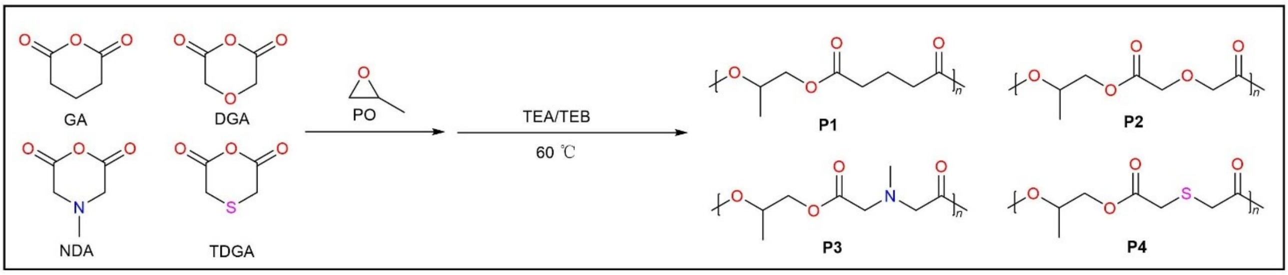

Scheme S1. Synthetic route of **P1~P4** catalyzed by TEA/TEB.

For **P1**. The resulting product was white. ^{1}H NMR (400 MHz, CDCl$_3$) δ 5.13 (d, J = 4.5 Hz, 1H), 4.18 (ddt, J = 10.0, 3.9, 2.1 Hz, 2H), 4.07 – 4.01 (m, 2H), 2.44 – 2.34 (m, 9H), 1.97 – 1.90 (m, 4H), 1.24 (d, J = 6.5 Hz, 6H). ^{13}C NMR (100 MHz, CDCl$_3$) δ 172.51, 68.21, 66.00, 33.31, 20.00, 16.51. The M_n, M_w from GPC Curves are 17.3 KDa and 25.7 KDa. PDI is 1.49.

For **P2**. The resulting product was light yellow. ^{1}H NMR (400 MHz, CDCl$_3$) δ 5.24 (d, J = 3.2 Hz, 1H), 4.31 – 4.11 (m, 11H), 1.29 (s, 4H). ^{13}C NMR (100 MHz, CDCl$_3$) δ 169.79, 69.29, 68.45, 66.57, 16.73. The M_n, M_w from GPC Curves are 8.74 KDa and 13.7 KDa. PDI is 1.57.

For **P3**. The resulting product was yellow. ^{1}H NMR (400 MHz, CDCl$_3$) δ 5.19 (s, 1H), 4.34 (d, J = 66.2 Hz, 1H), 4.05 (s, 2H), 2.51 (q, J = 6.2 Hz, 20H), 1.35 – 1.18 (m, 35H). ^{13}C NMR (100 MHz, CDCl$_3$) δ 170.60, 68.56, 66.10, 57.28, 42.14, 25.73, 16.67. The M_n, M_w from GPC Curves are 1.52 KDa and 3.10 KDa. PDI is 2.03.

For **P4**. The resulting product was deep red. ^{1}H NMR (400 MHz, CDCl$_3$) δ 5.17 (s, 1H), 4.25 (d, J = 8.6 Hz, 1H), 4.14 (s, 1H), 3.38 (s, 3H), 1.28 (s, 2H), 1.27 – 1.18 (m, 1H). ^{13}C NMR (100 MHz, CDCl$_3$) δ 169.30, 69.13, 66.46, 33.43, 16.13. The M_n, M_w from GPC Curves are 3.90 KDa and 6.63 KDa. PDI is 1.70.

Synthesis of P1, P2, and P4 catalyzed by Zn-Co(Ⅲ) DMCC.

In a glovebox, Zn-Co(Ⅲ) DMCC (2.0 mg), PO (0.28 ml, 4.0 mmol), and toluene (2.0 mL) were measured into three 35.0 mL vials equipped with Teflon-coated stir bars. GA (912 mg, 8.0 mmol), DGA (928 mg, 8.0 mmol), and TDGA (1056 mg, 8.0 mmol) were added via syringes, washing all solids into the base of the three vials, respectively. The three vials were sealed with a Teflon-lined cap, removed from the glovebox, and immersed into an oil-bath preheated to 80 ℃. After 72 h reaction, the solution became viscous and transparent. The three vials were then removed from the heat block and cooled to room temperature. The mixtures of the six vials were dissolved in 1.5 mL DCM, filtered through a 0.22-micron organic filter head, and then put into ca. 50 mL analytical ethanol (without PL response) to precipitate the products, respectively. The dissolve-precipitation process was repeated three times to remove unreacted monomers and catalysts. The polymers were finally collected and dried in vacuum at 45 ℃ for 12 h.

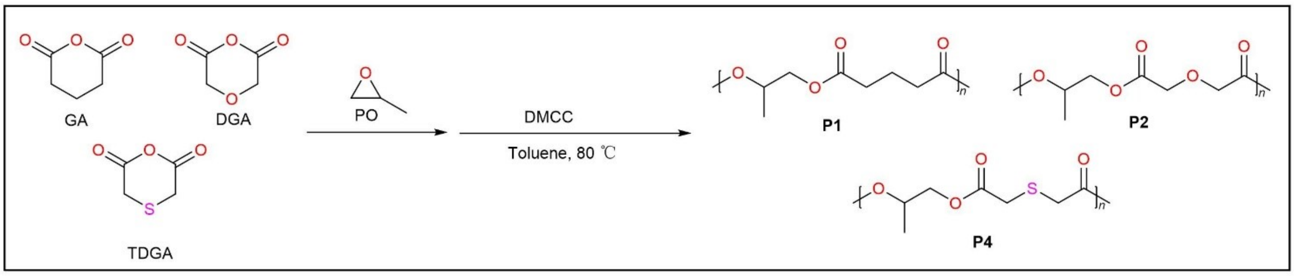

Scheme S2. Synthetic route of **P1**, **P2,** and **P4** catalyzed by Zn-Co(Ⅲ) DMCC.

For **P1**. The resulting product was white. ^{1}H NMR (400 MHz, $CDCl_3$) δ 5.13 (s, 1H), 4.18 (s, 0H), 4.04 (s, 1H), 2.38 (s, 1H), 1.93 (s, 1H), 1.25 (s, 2H).^{13}C NMR (100 MHz, $CDCl_3$) δ 172.66, 68.36, 66.16, 33.47, 20.16, 16.67. The M_n, M_w from GPC Curves are 12.9 KDa and 29.5 KDa. PDI is 2.28.

For **P2**. The resulting product was light yellow. ^{1}H NMR (400 MHz, $CDCl_3$) δ 5.24 (s, 1H), 4.31 (s, 3H), 4.22 (s, 10H), 4.13 (s, 1H), 1.28 (s, 7H). ^{13}C NMR (100 MHz, $CDCl_3$) δ 169.57, 69.07, 68.03, 66.35, 16.51. The M_n, M_w from GPC Curves are 4.32 KDa and 4.88 KDa. PDI is 1.12.

For **P4**. The resulting product was deep red. ^{1}H NMR (400 MHz, $(CD_3)_2SO$) δ 5.06 (s, 1H), 4.24 – 4.05 (m, 7H), 3.46 (d, J = 27.5 Hz, 4H), 1.32 – 1.02 (m, 44H). ^{13}C NMR (100 MHz, $(CD_3)_2SO$) δ 169.30, 68.96, 66.03, 33.02 (d, J = 27.8 Hz), 15.85. The M_n, M_w from GPC Curves are 3.51 KDa and 5.75 KDa. PDI is 1.64.

Computational Details

All the calculations were performed with density functional theory (DFT) and time-dependent density functional theory (TDDFT) implemented in Gaussian 09 program package. The polymer-related calculations were replaced by the oligomers with five repeating units and the ground state equilibrium geometries and the normal modes of vibration were computed using the hybrid functional B3LYP, together basis set 6-31G(d). Time-dependent density functional theory (TD-DFT) was utilized at the same level of theory to calculate optimized excited (S1) geometries. The frontier molecular orbitals (FMO) of **P1~P4** were displayed using IQmol molecular viewer package (Isovalue: 0.02). In addition, the model molecules M1~M7 in gas phase were also optimized at wb97XD/6-31+G(d) level. Analytical frequency calculations were also performed at the same level of theory to confirm that the optimized structures were at a minimum point. Time-dependent density functional theory (TD-DFT) was utilized at the same level of theory to calculate optimized excited (S1) geometries. The frontier molecular orbitals (FMO) of M1~M7 were displayed using Visual Molecular Dynamics (VMD)[1] (Isovalue: 0.003). Hole-electron analyses[2] were calculated by Multiwfn 3.8[3] and were displayed using Visual Molecular Dynamics (VMD) (Isovalue: 0.002). Interfragment charge transfer (IFCT) was well used to quantify the mutual charge transfer between carbonyl groups and heteroatoms upon the excited state.

NMR Spectra

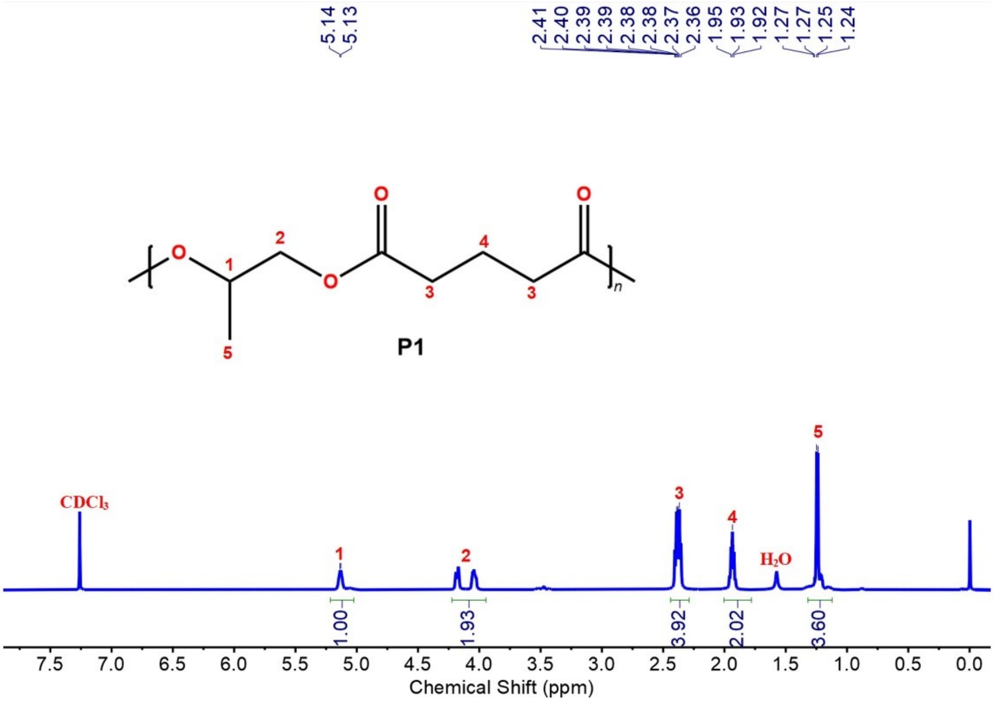

Figure S1. ^{1}H NMR spectra of polyester **P1** catalyzed by TEA/TEB (400 MHz, $CDCl_3$).

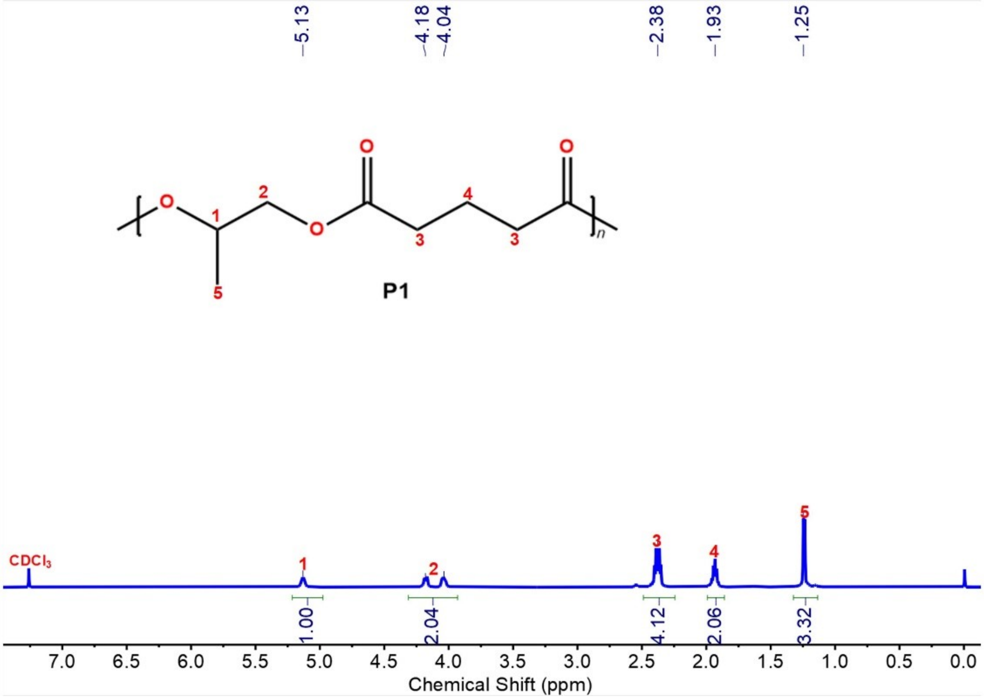

Figure S2. ^{1}H NMR spectra of polyester **P1** catalyzed by DMCC (400 MHz, $CDCl_3$).

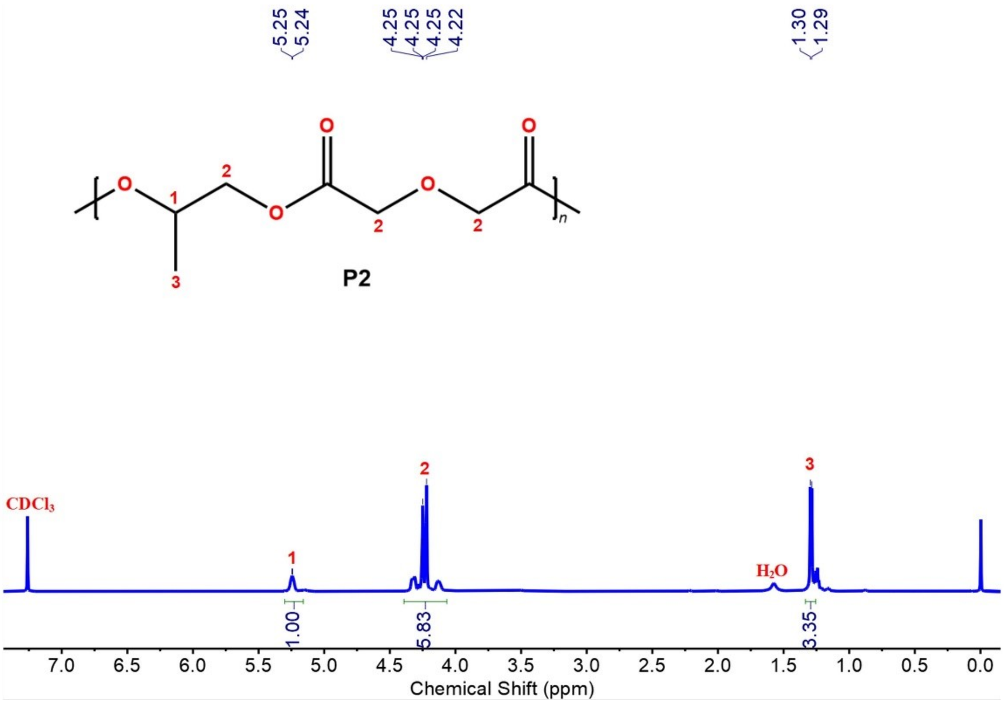

Figure S3 ^{1}H NMR spectra of polyester **P2** catalyzed by TEA/TEB. (400 MHz, $CDCl_3$).

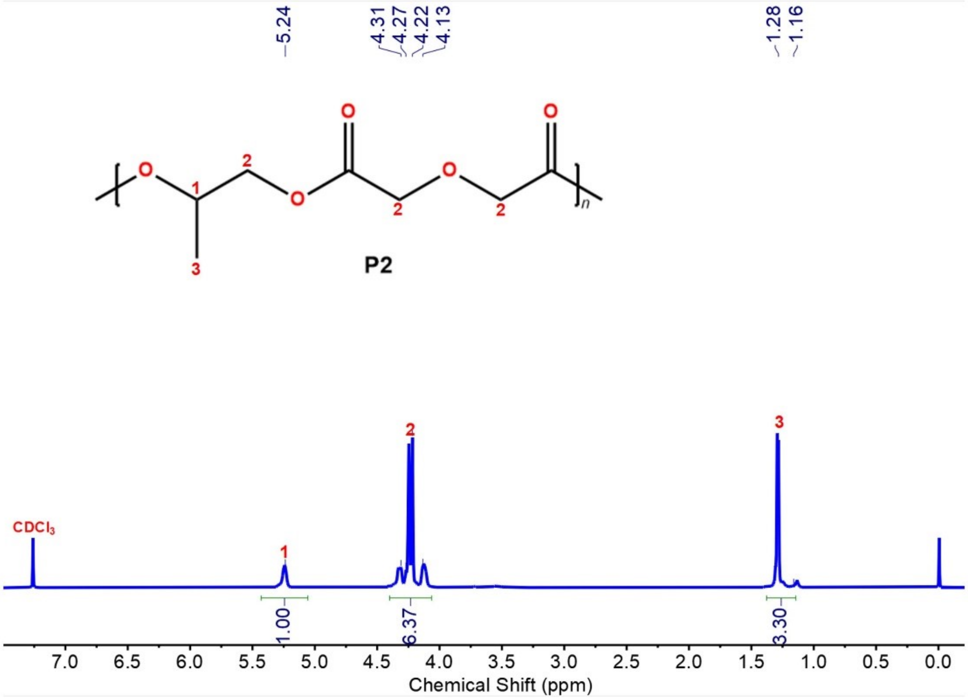

Figure S4. ^{1}H NMR spectra of polyester **P2** catalyzed by DMCC (400 MHz, $CDCl_3$).

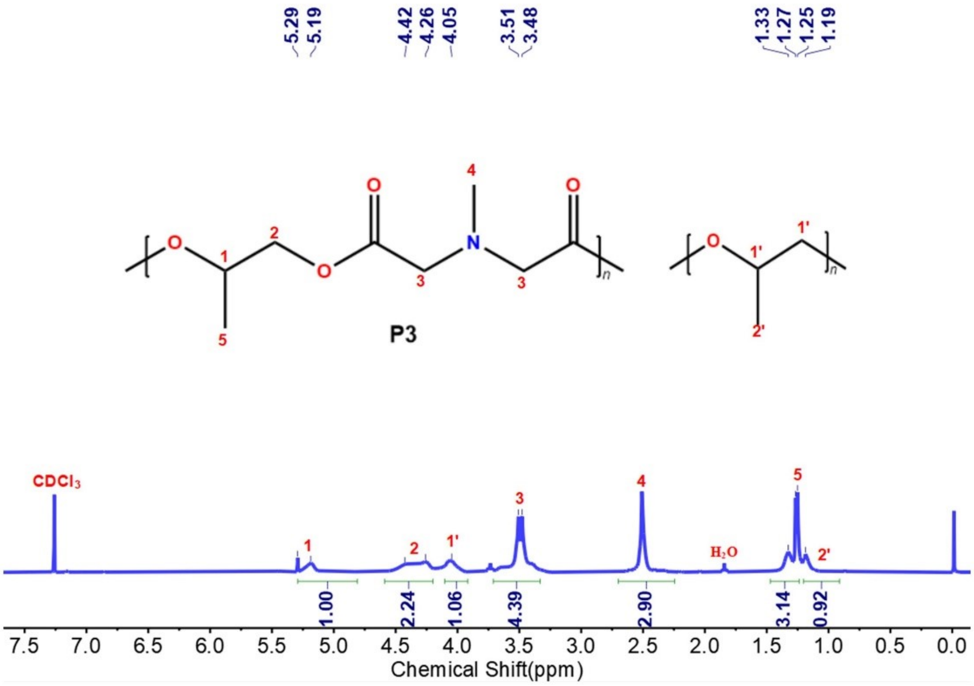

Figure S5. ^{1}H NMR spectra of polyester **P3** catalyzed by TEA/TEB (400 MHz, $CDCl_3$).

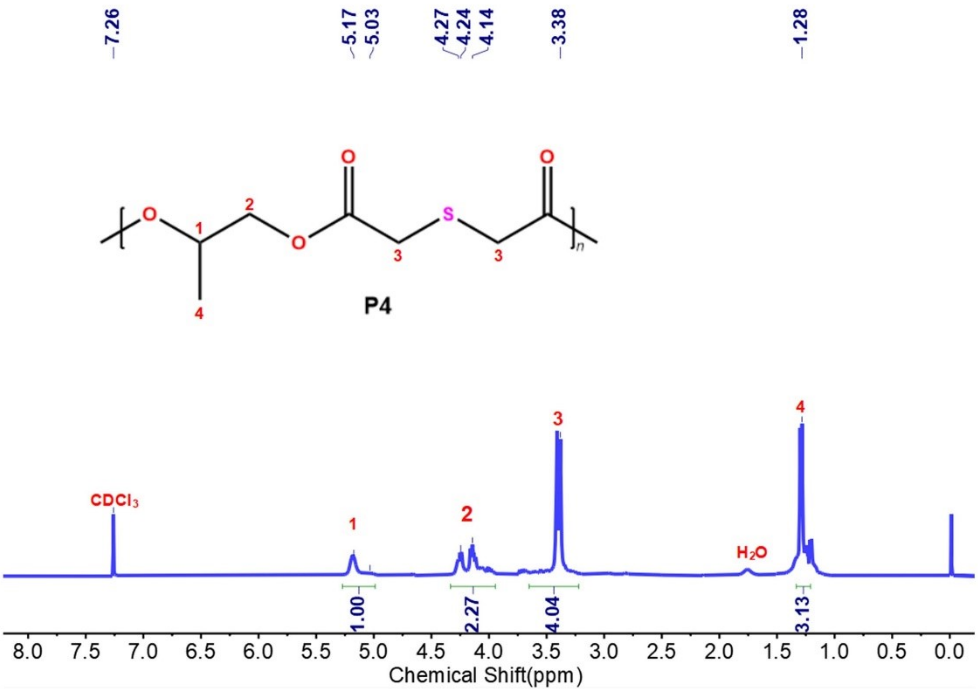

Figure S6. ^{1}H NMR spectra of polyester **P4** catalyzed by TEA/TEB (400 MHz, $CDCl_3$).

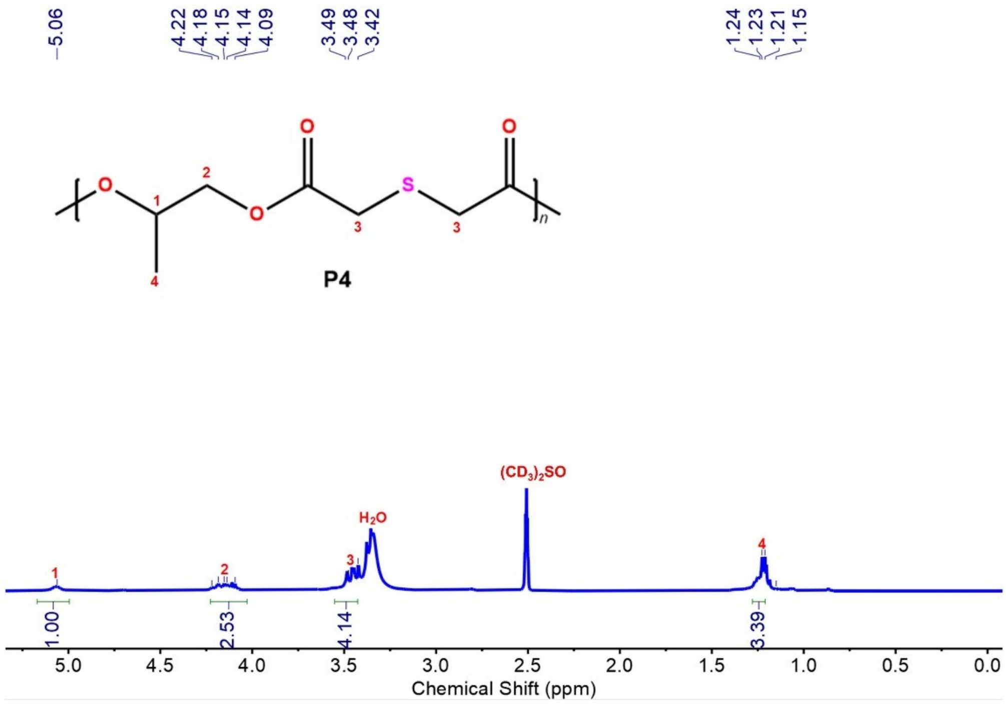

Figure S7. ^{1}H NMR spectra of polyester **P4** catalyzed by DMCC (400 MHz,$(CD_3)_2SO$).

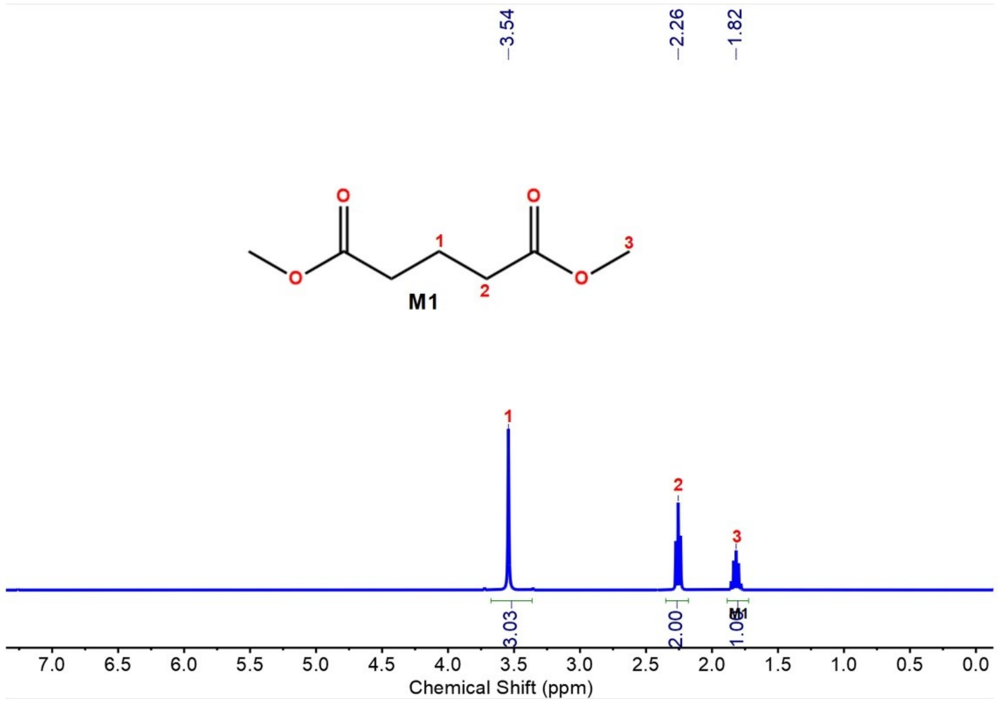

Figure S8. ^{1}H NMR spectra of M1 (400 MHz, $CDCl_3$, δ 3.54 (s, 7H), 2.26 (s, 2H), 1.82 (s, 1H)).

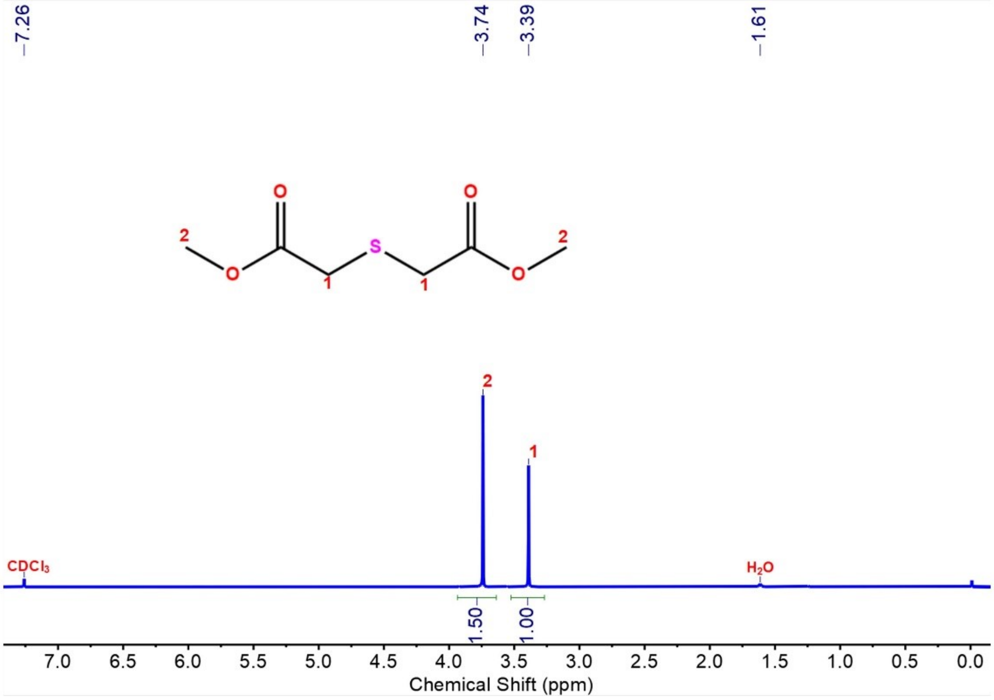

Figure S9. ^{1}H NMR spectra of M2 (400 MHz, $CDCl_3$, δ 3.74 (s, 1H), 3.39 (s, 1H)).

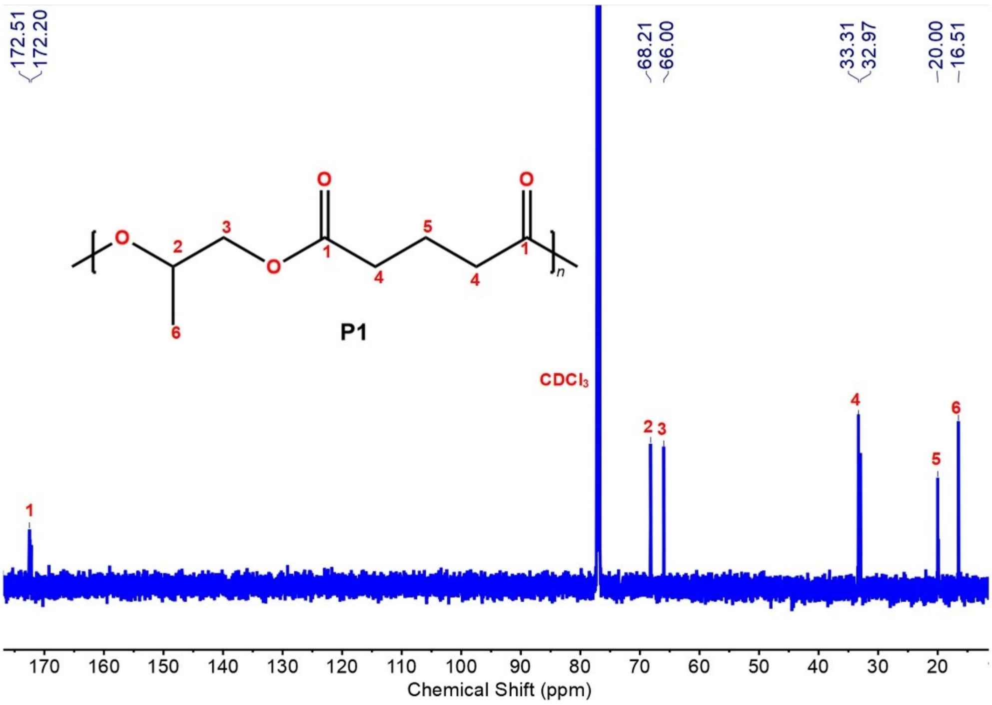

Figure S10. ^{13}C NMR spectra of polyester **P1** catalyzed by TEA/TEB (100 MHz, $CDCl_3$).

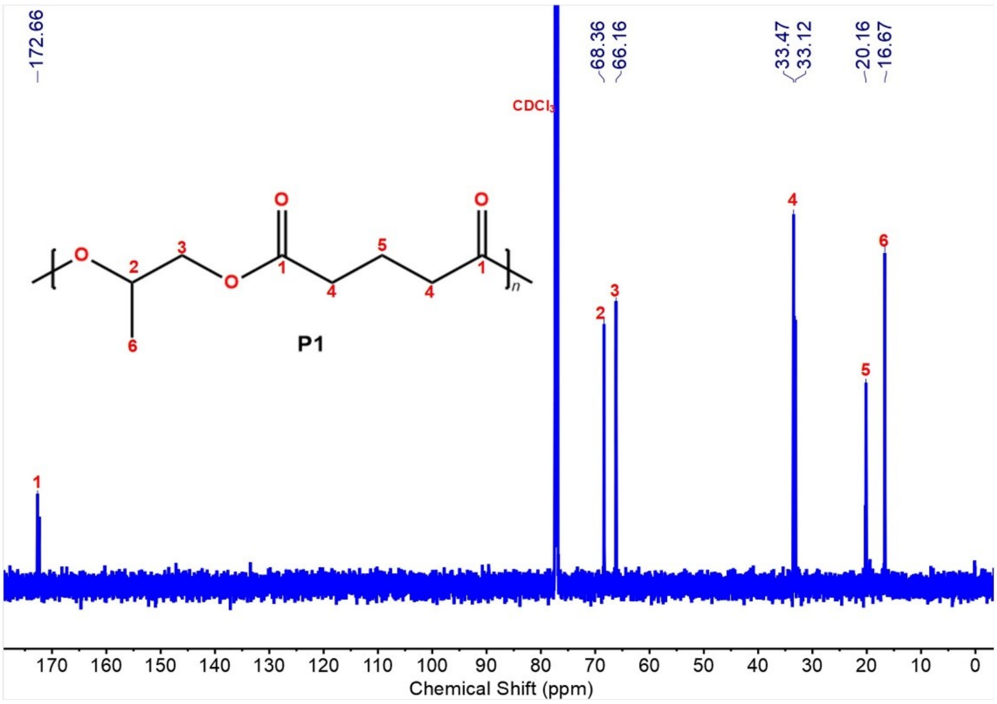

Figure S11. ^{13}C NMR spectra of polyester **P1** catalyzed by DMCC (100 MHz, $CDCl_3$).

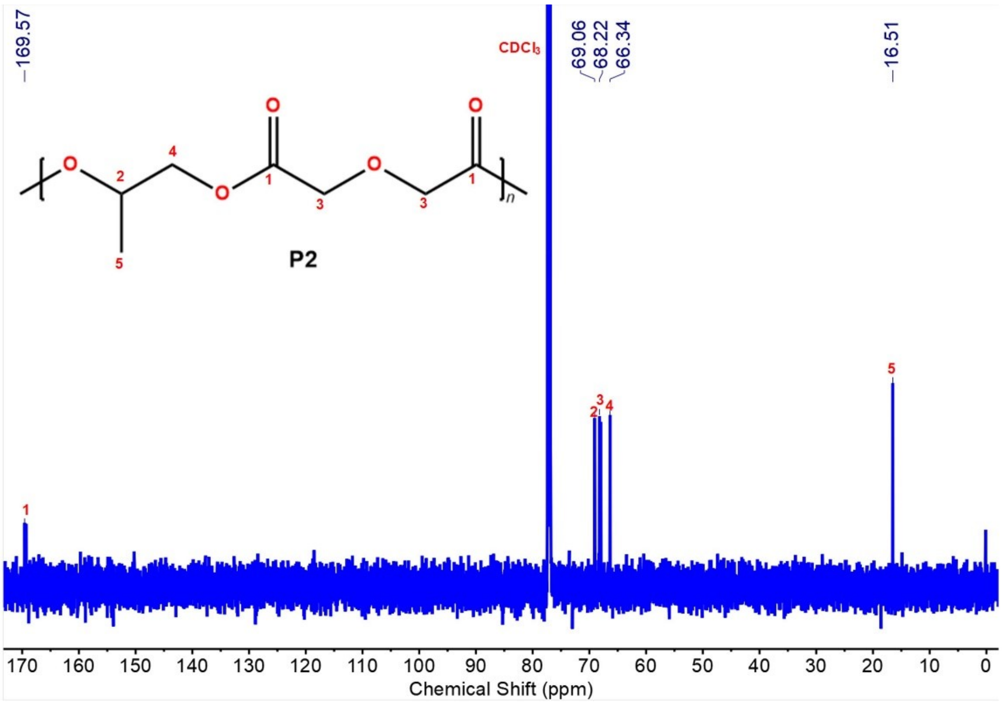

Figure S12. ^{13}C NMR spectra of polyester **P2** catalyzed by TEA/TEB (100 MHz, $CDCl_3$).

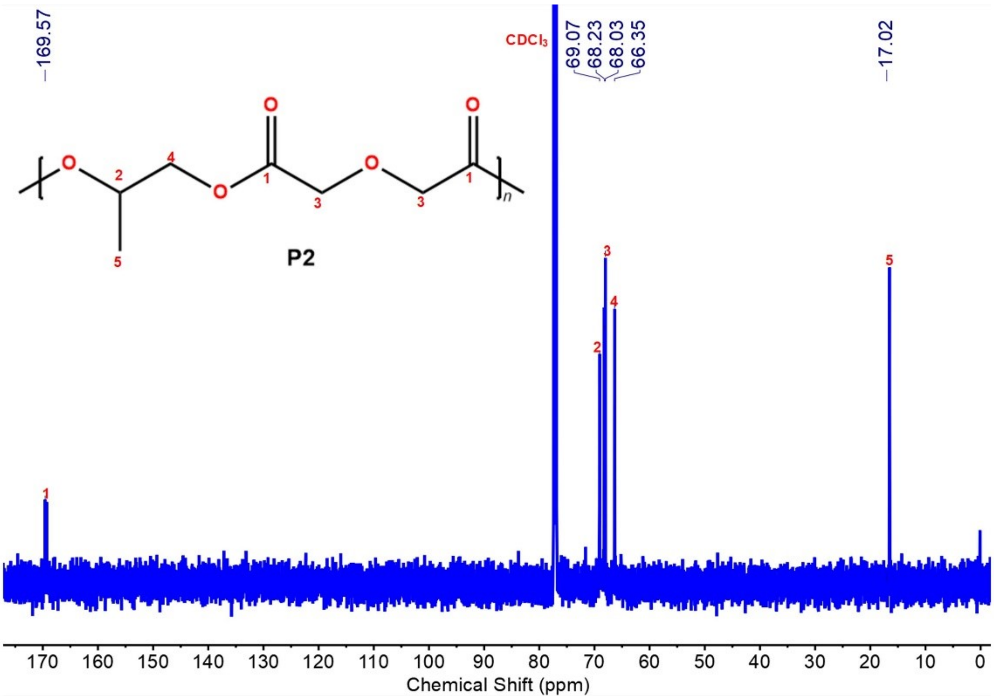

Figure S13. ^{13}C NMR spectra of polyester **P2** catalyzed by DMCC (100 MHz, $CDCl_3$).

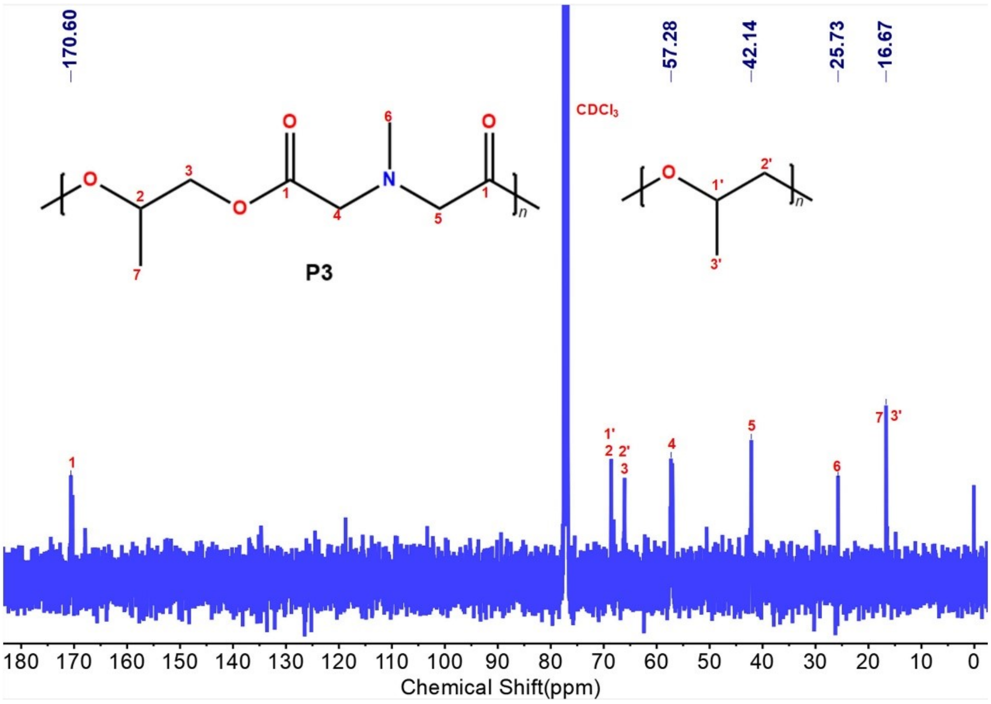

Figure S14. ^{13}C NMR spectra of polyester **P3** catalyzed by TEA/TEB (100 MHz, $CDCl_3$).

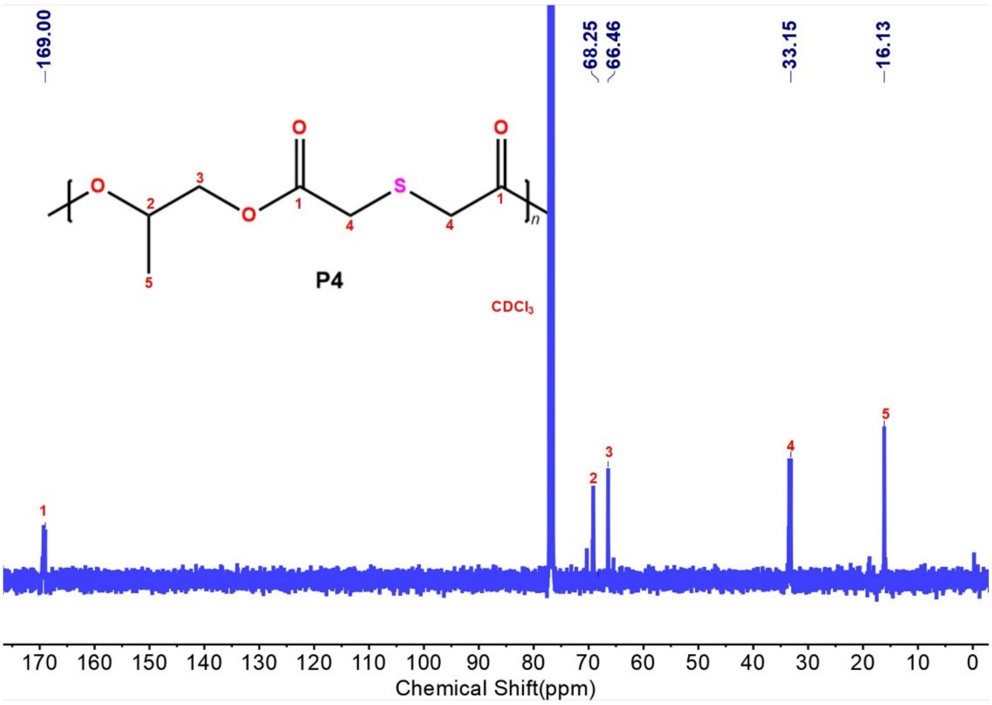

Figure S15. ^{13}C NMR spectra of polyester **P4** catalyzed by TEA/TEB (100 MHz, $CDCl_3$).

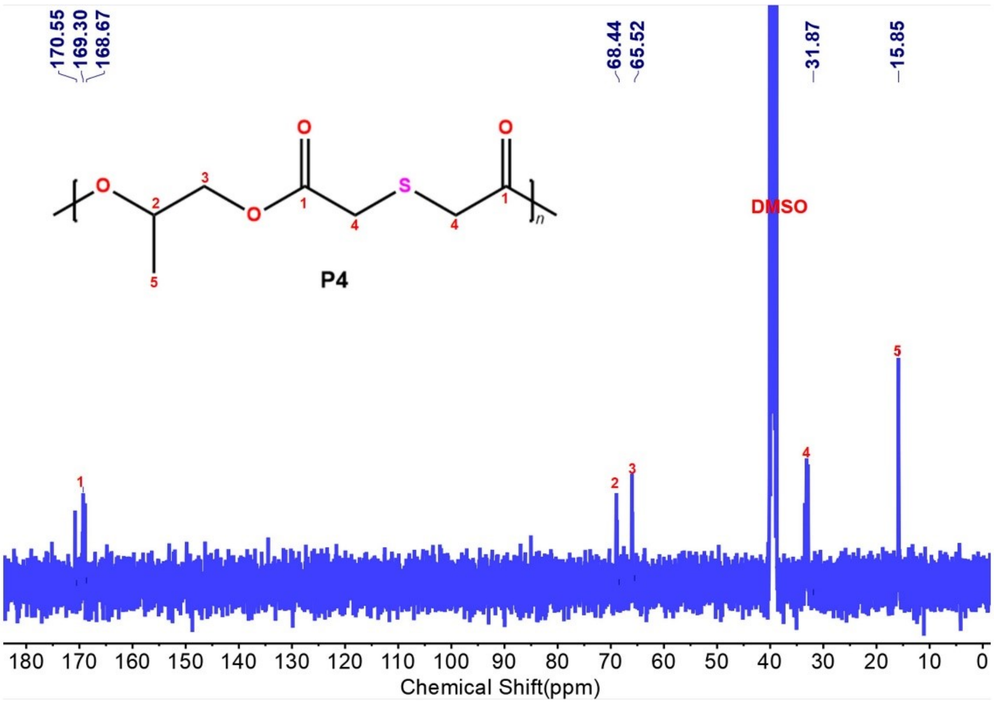

Figure S16. ^{13}C NMR spectra of polyester **P4** catalyzed by DMCC (100 MHz, $(CD_3)_2SO$).

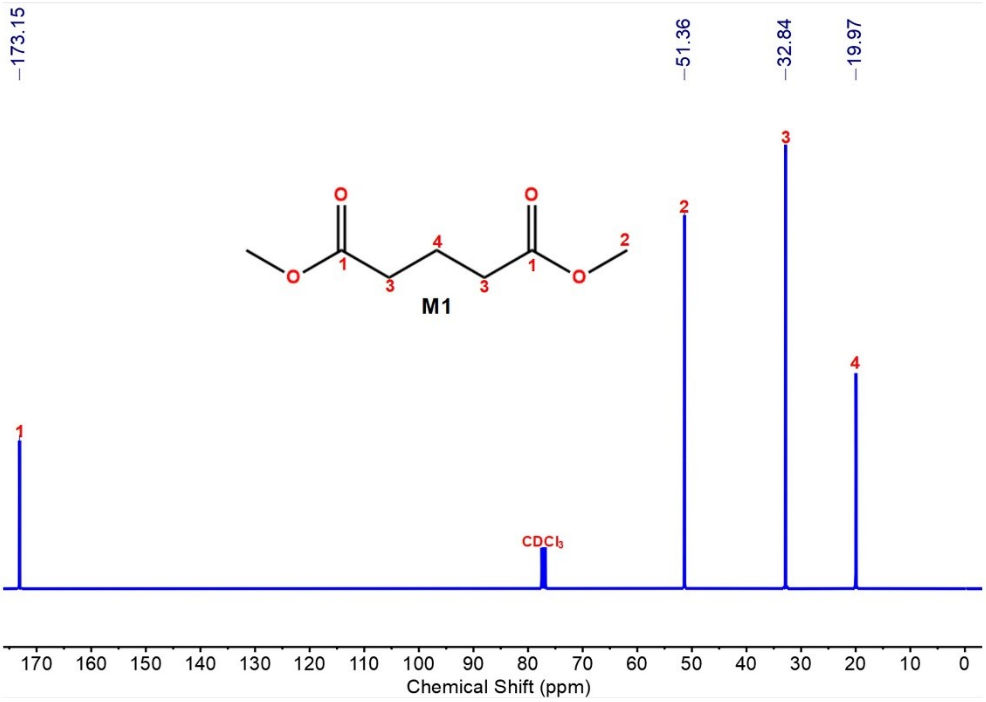

Figure S17. ${}^{13}C$ NMR spectra of M1 (100 MHz, CDCl3, *δ* 173.15, 51.36, 32.84, 19.97).

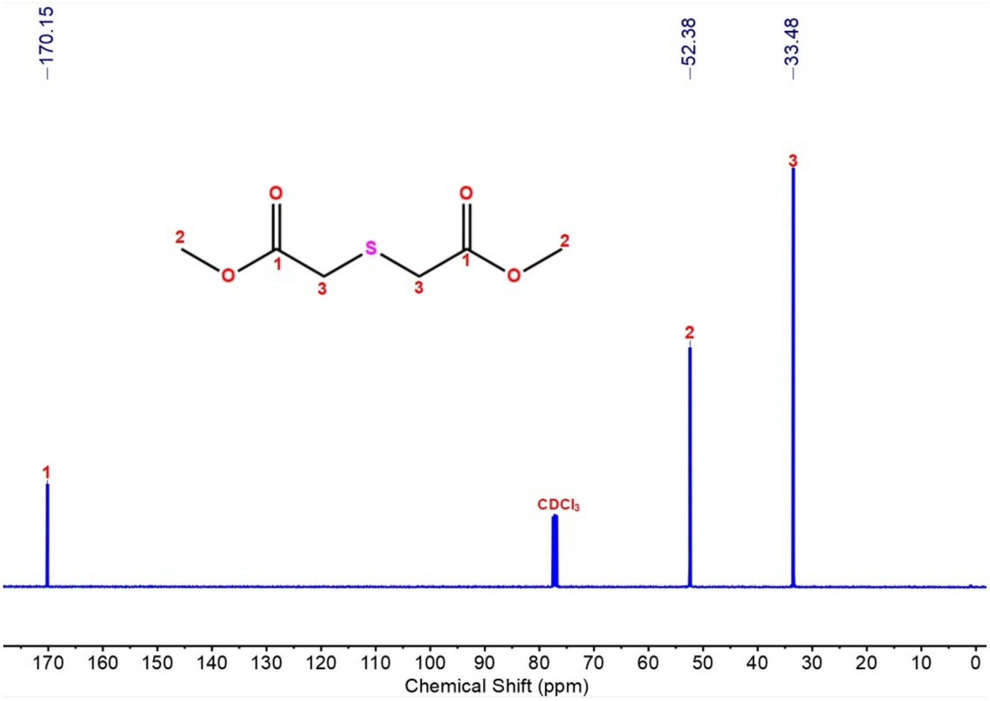

Figure S18. ${}^{13}C$ NMR spectra of M2 (100 MHz, CDCl3, *δ* 170.15, 52.38, 33.48).

Gel Permeation Chromatography

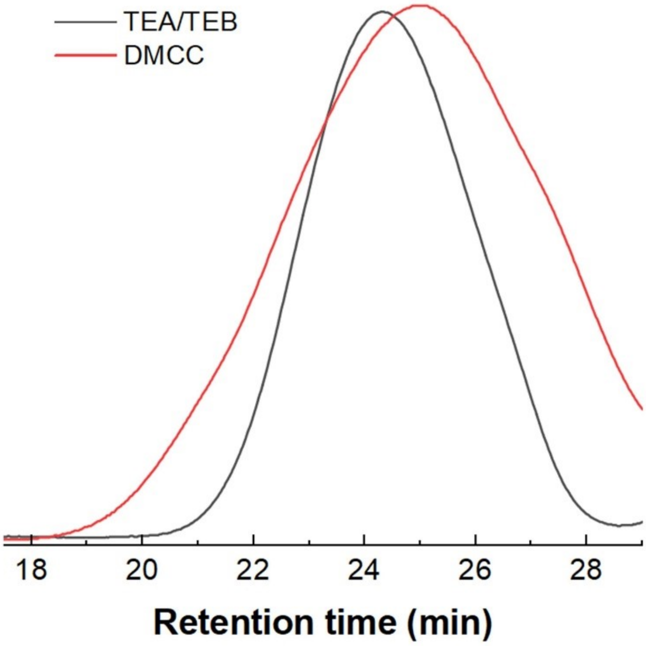

Figure S19. GPC curves of **P1** catalyzed by TEA/TEB and DMCC, respectively.

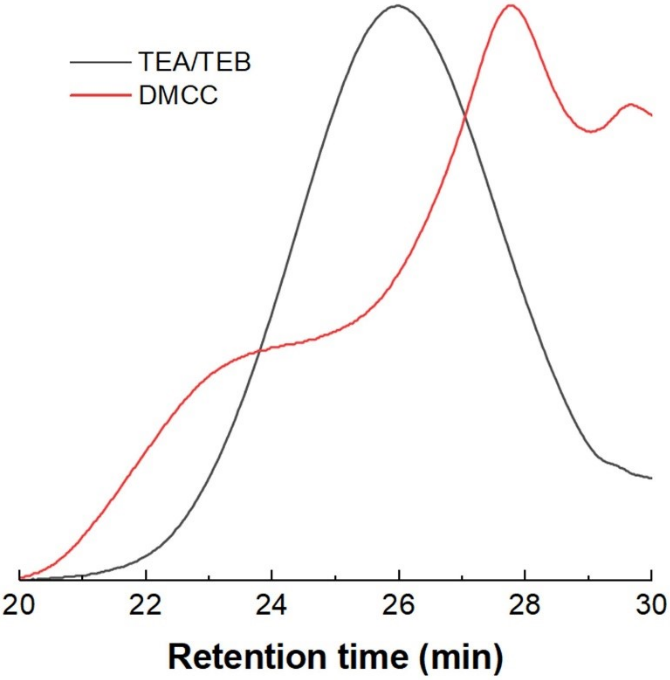

Figure S20. GPC curves of **P2** catalyzed by TEA/TEB and DMCC, respectively.

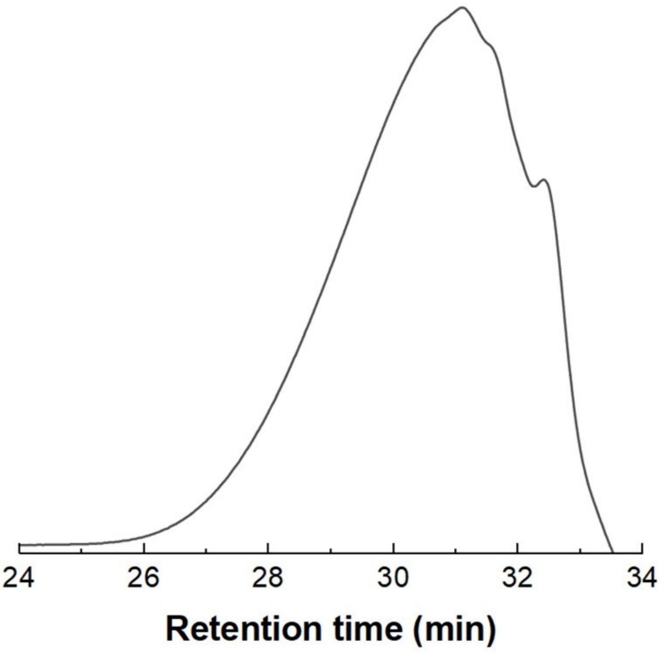

Figure S21. GPC curve of **P3** catalyzed by TEA/TEB.

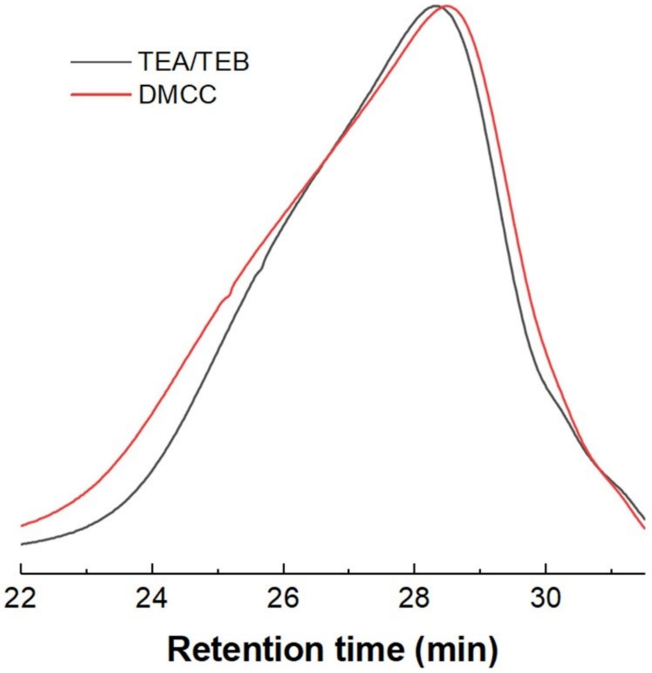

Figure S22. GPC curves of **P4** catalyzed by TEA/TEB and DMCC, respectively.

MALDI-TOF mass spectra

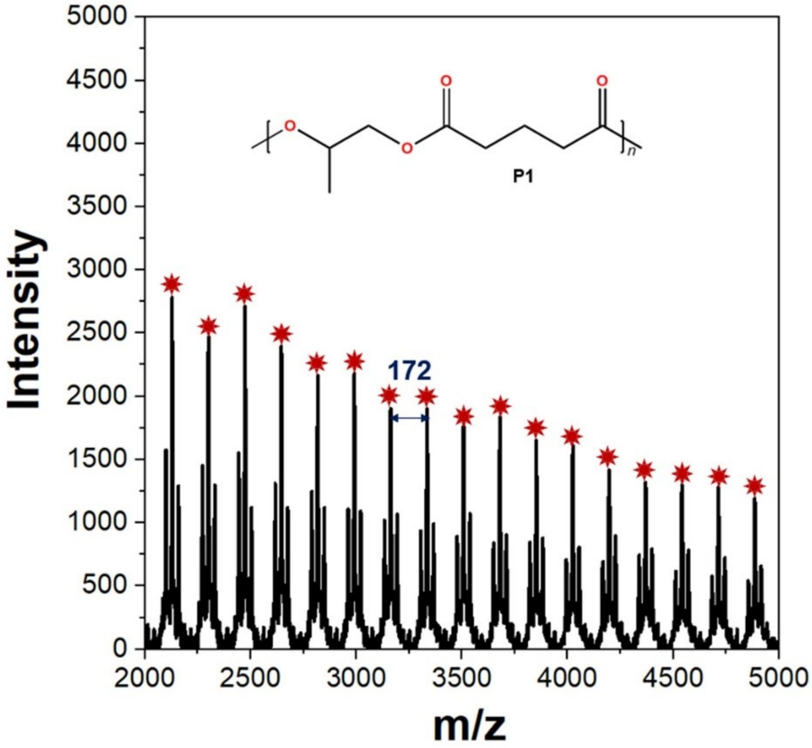

Figure S23. MALDI-TOF MS of **P1**. "172" is the sum molar masses of GA (114 g/mol) and PO (58 g/mol).

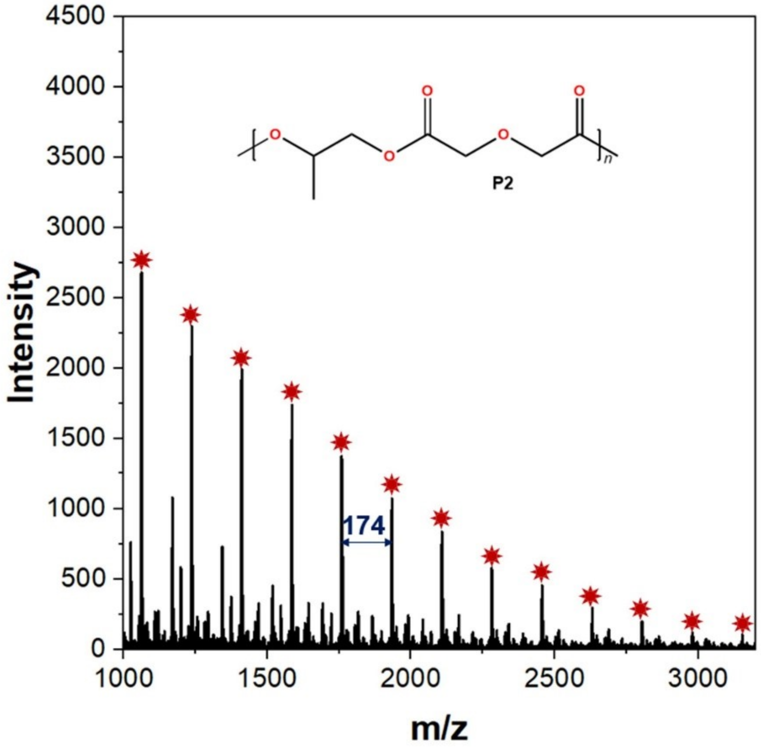

Figure S24. MALDI-TOF MS of **P2**. "174" is the sum molar masses of DGA (116 g/mol) and PO (58 g/mol).

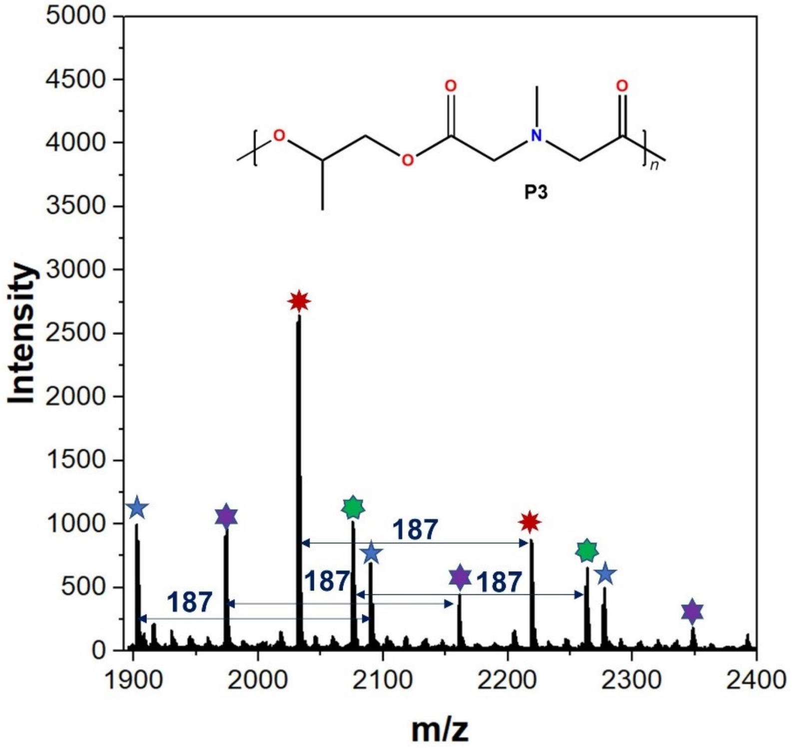

Figure S25. MALDI-TOF MS of **P3**. “187” is the sum molar masses of NDA (129 g/mol) and PO (58 g/mol).

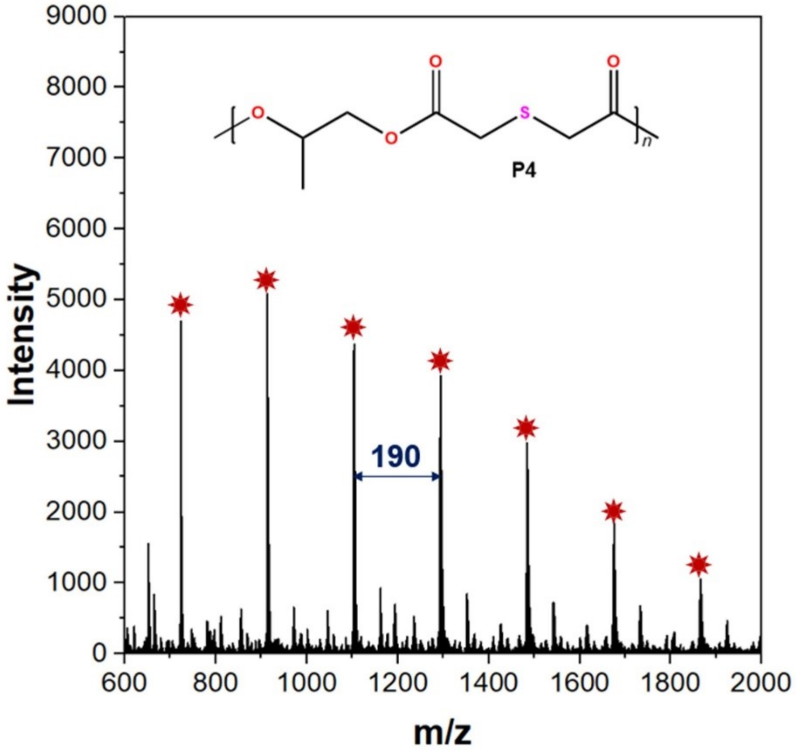

Figure S26. MALDI-TOF MS of **P4**. “190” is the sum molar masses of TDGA (132 g/mol) and PO (58 g/mol).

Supplemental photophysical characterization

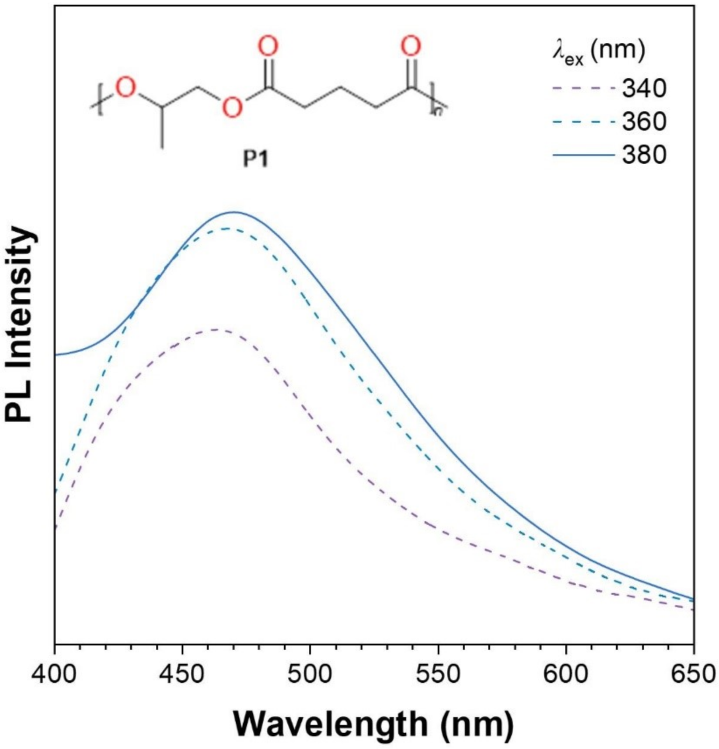

Figure S27. Photoluminescent (PL) spectra of **P1** catalyzed by TEA/TEB in solid with different excitation wavelengths (λ_{ex}).

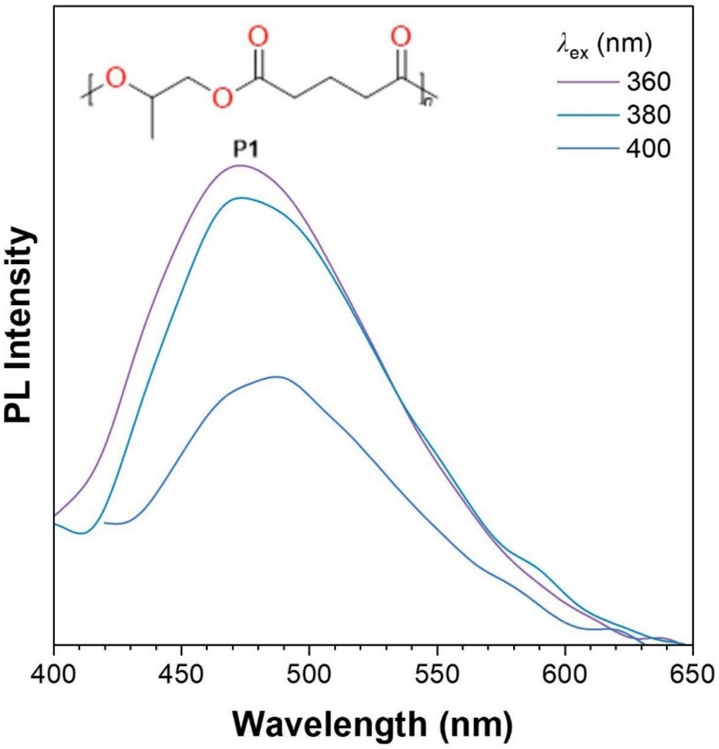

Figure S28. PL spectra of **P1** catalyzed by DMCC in solid with different λ_{ex}.

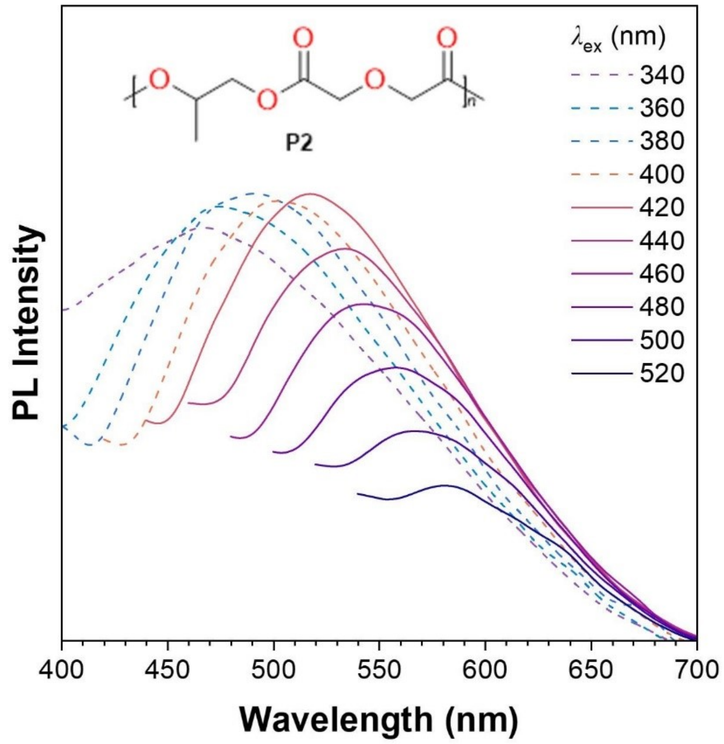

Figure S29. PL spectra of **P2** catalyzed by TEA/TEB in solid with different λ_{ex}.

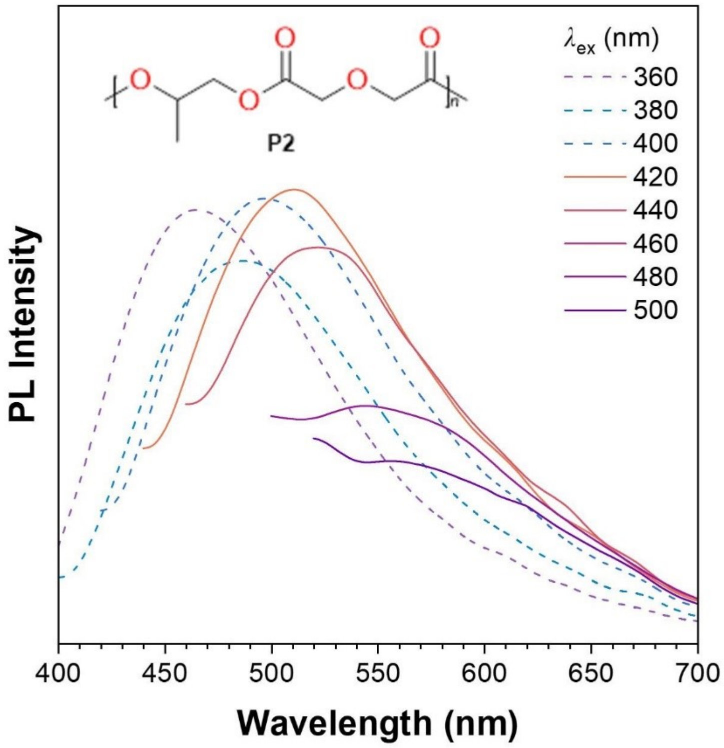

Figure S30. PL spectra of **P2** catalyzed by DMCC in solid with different λ_{ex}.

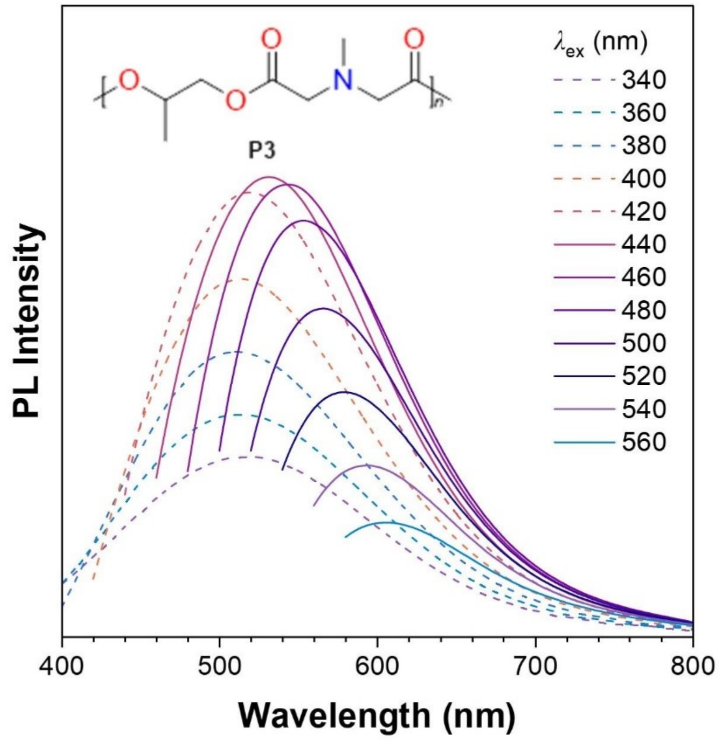

Figure S31. PL spectra of **P3** catalyzed by TEA/TEB in solid with different λ_{ex}.

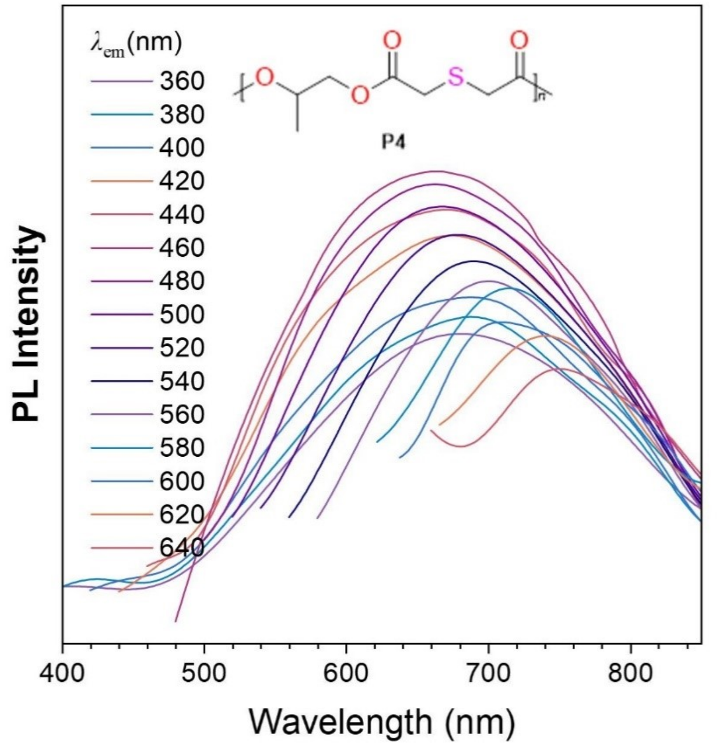

Figure S32. PL spectra of **P4** catalyzed by TEA/TEB in solid with different λ_{ex}.

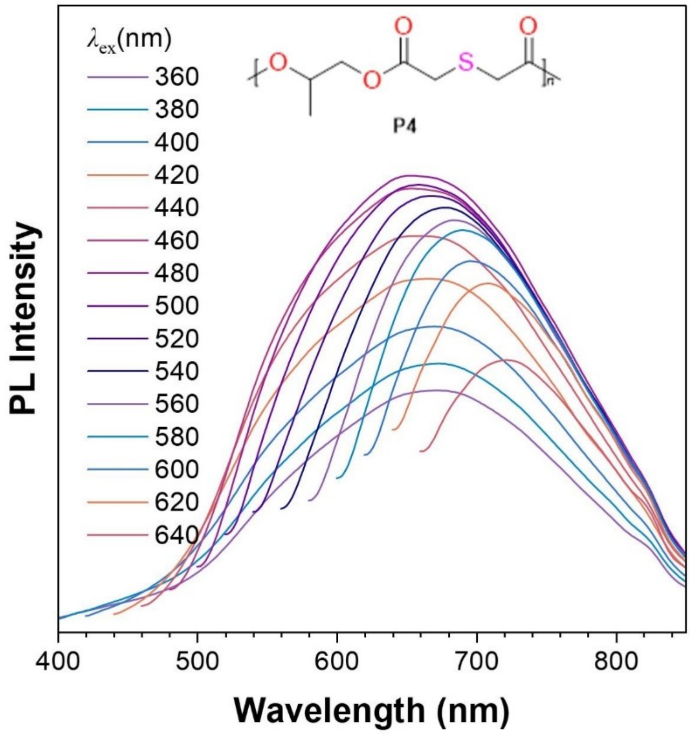

Figure S33. PL spectra of **P4** catalyzed by DMCC in solid with different λ_{ex}.

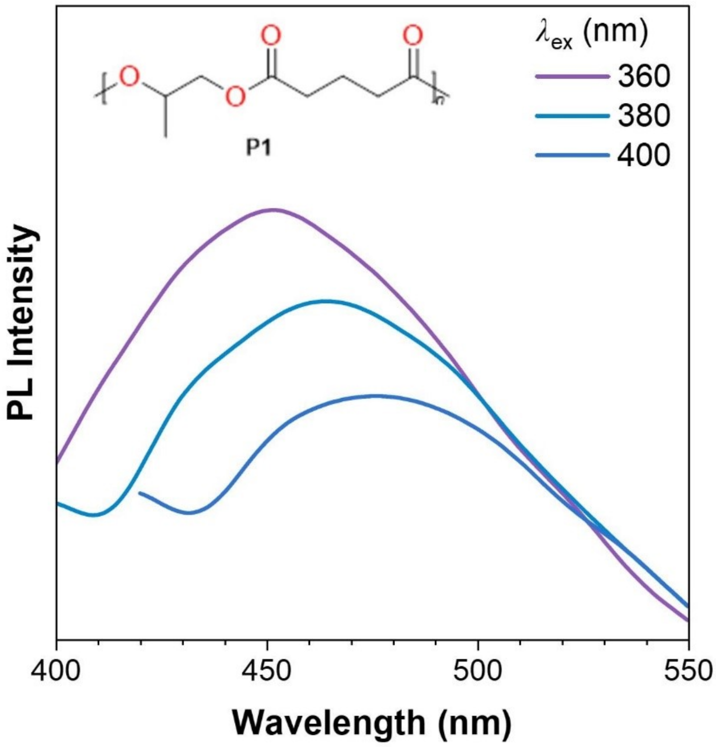

Figure S34. PL spectra of **P1** catalyzed by TEA/TEB in DCM (c = 10^{-1} M) with different λ_{ex}.

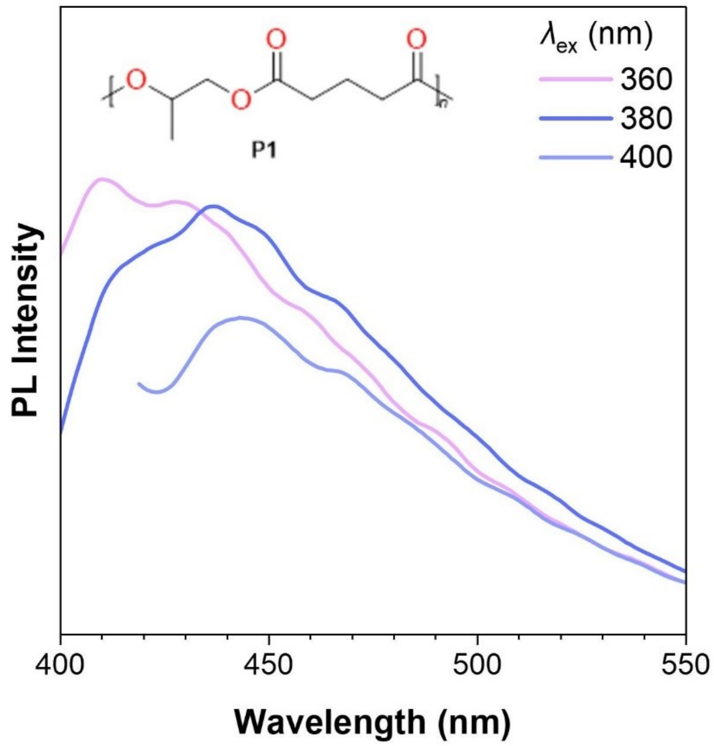

Figure S35. PL spectra of **P1** catalyzed by DMCC in DCM ($c = 10^{-1}$ M) with different λ_{ex}.

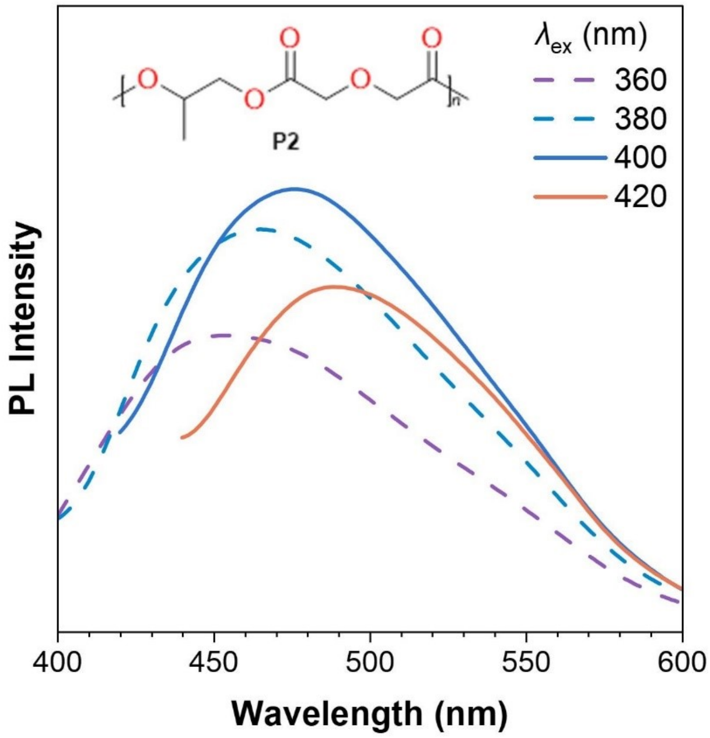

Figure S36. PL spectra of **P2** catalyzed by TEA/TEB in DCM ($c = 10^{-1}$ M) with different λ_{ex}.

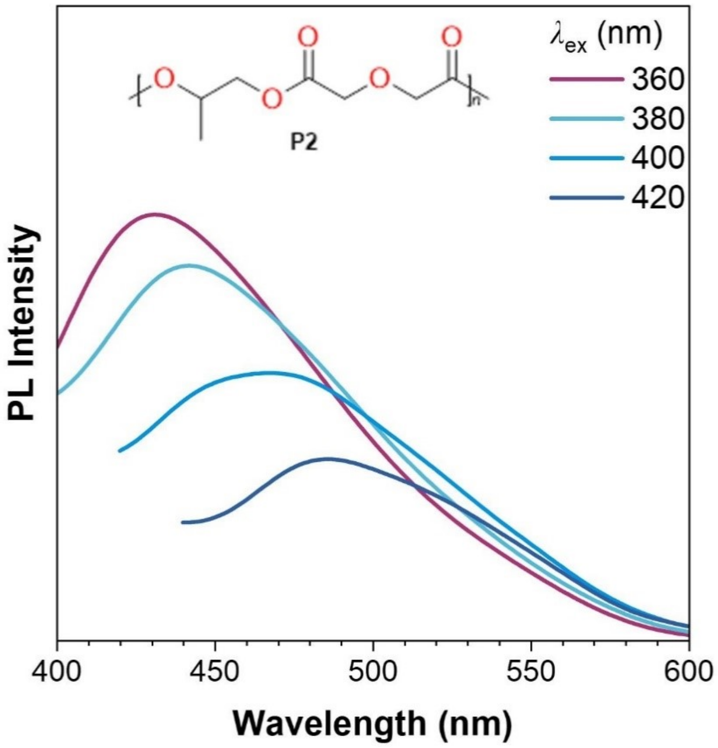

Figure S37. PL spectra of **P2** catalyzed by DMCC in DCM ($c = 10^{-1}$ M) with different λ_{ex}.

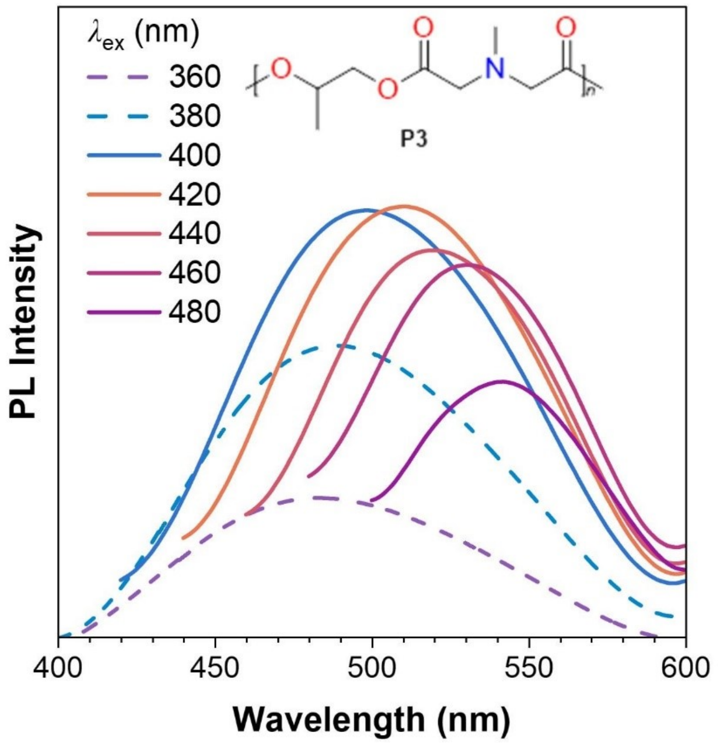

Figure S38. PL spectra of **P3** catalyzed by TEA/TEB in DCM ($c = 10^{-1}$ M) with different λ_{ex}.

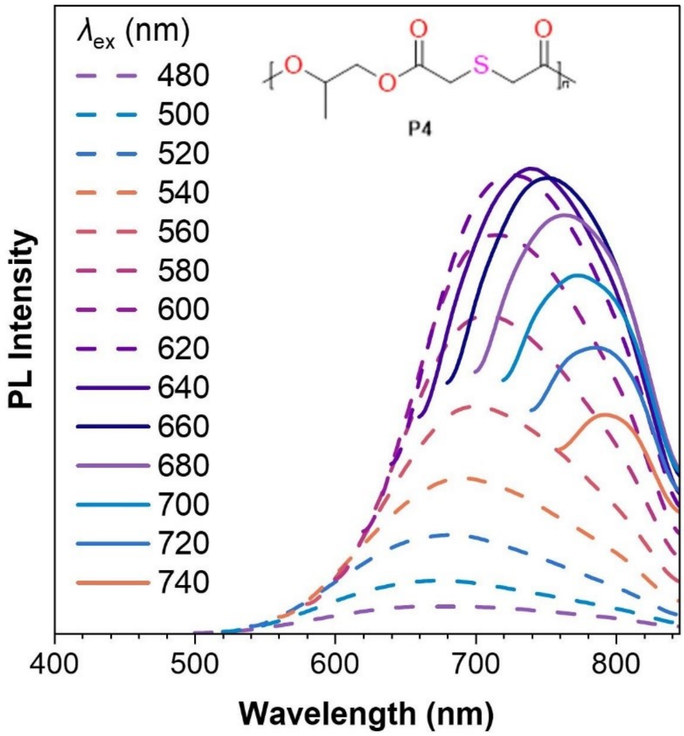

Figure S39. PL spectra of **P4** catalyzed by TEA/TEB in DCM (c = 10^{-1} M) with different λ_{ex}.

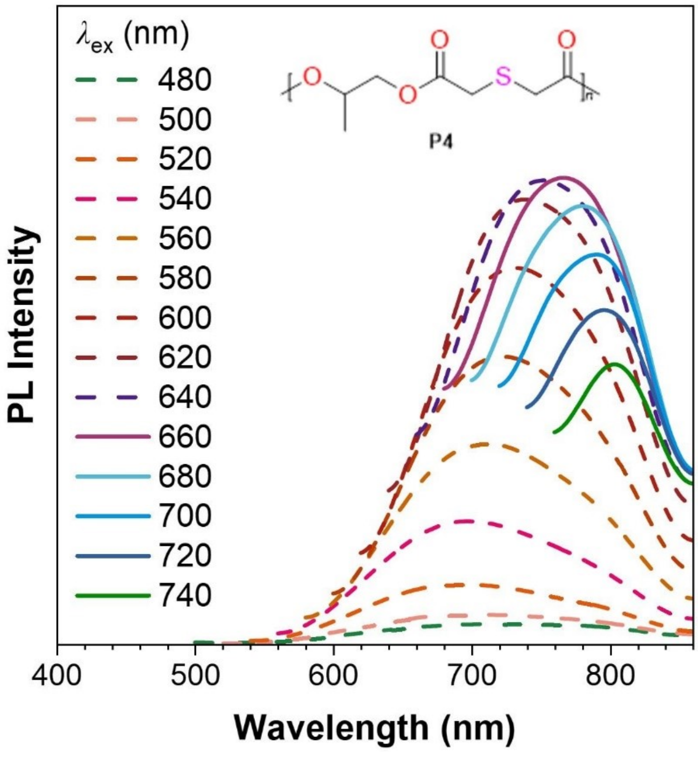

Figure S40. PL spectra of **P4** catalyzed by DMCC in DCM (c = 10^{-1} M) with different λ_{ex}.

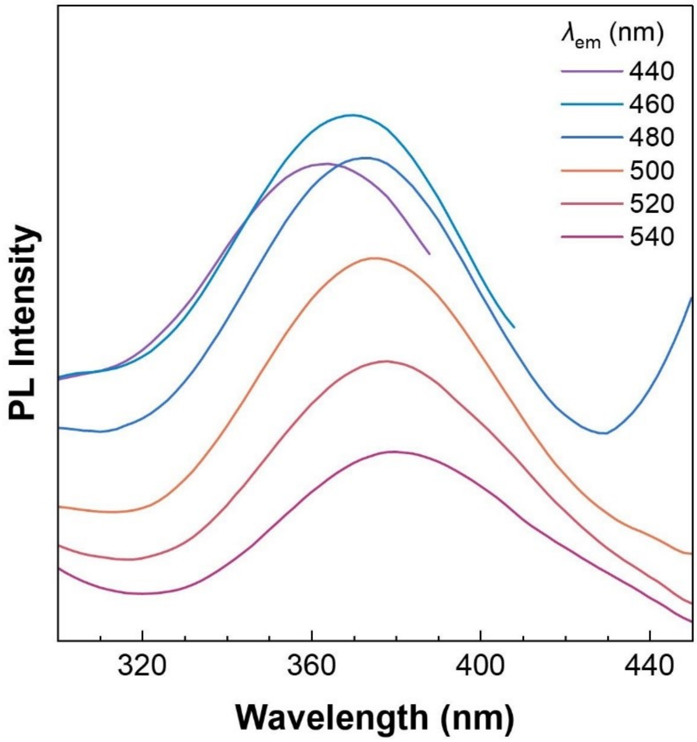

Figure S41. Excitation (EX) spectra of **P1** catalyzed by TEA/TEB in solid with different λ_{em}.

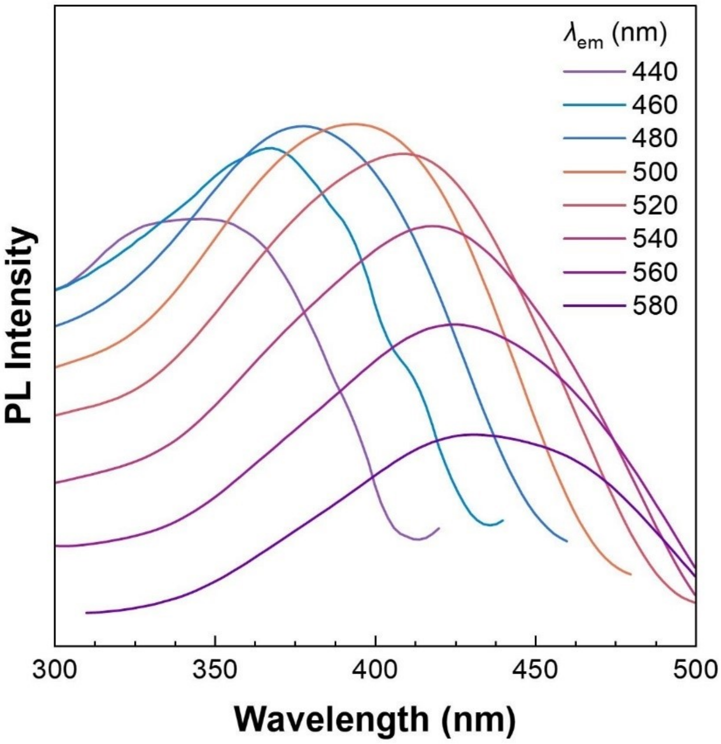

Figure S42. EX spectra of **P2** catalyzed by TEA/TEB in solid with different λ_{em}.

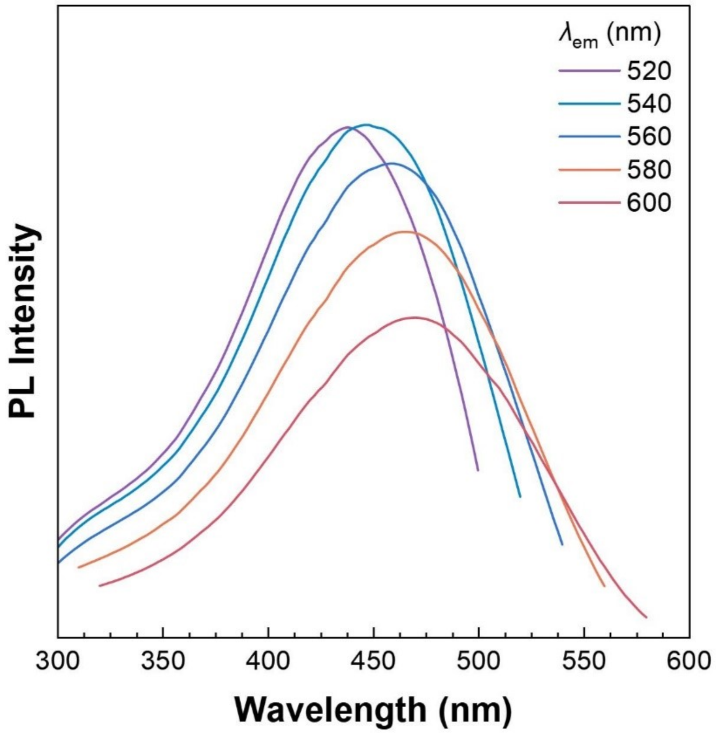

Figure S43. EX spectra of **P3** catalyzed by TEA/TEB in solid with different λ_{em}.

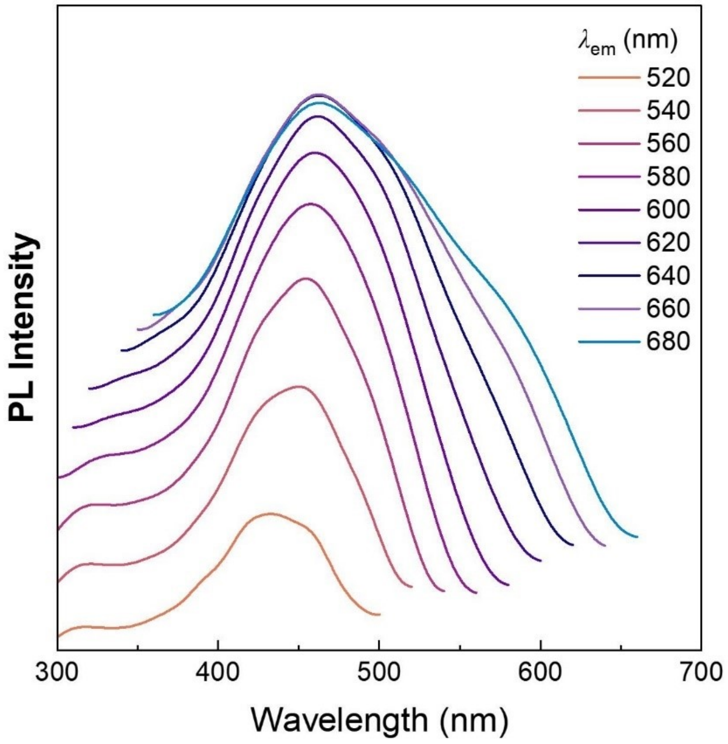

Figure S44. EX spectra of **P4** catalyzed by TEA/TEB in solid with different λ_{em}.

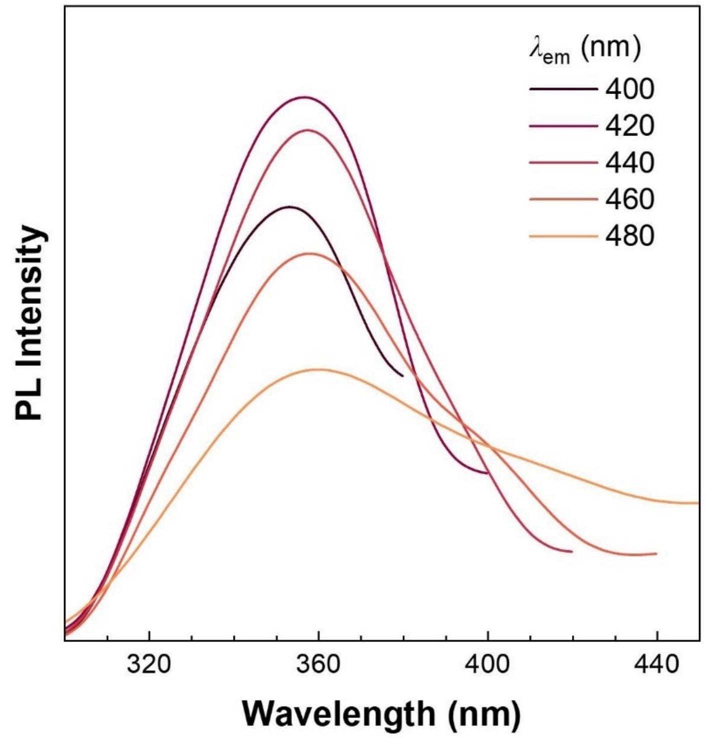

Figure S45. EX spectra of **P1** catalyzed by TEA/TEB in DCM (c = 10^{-1} M) with different λ_{em}.

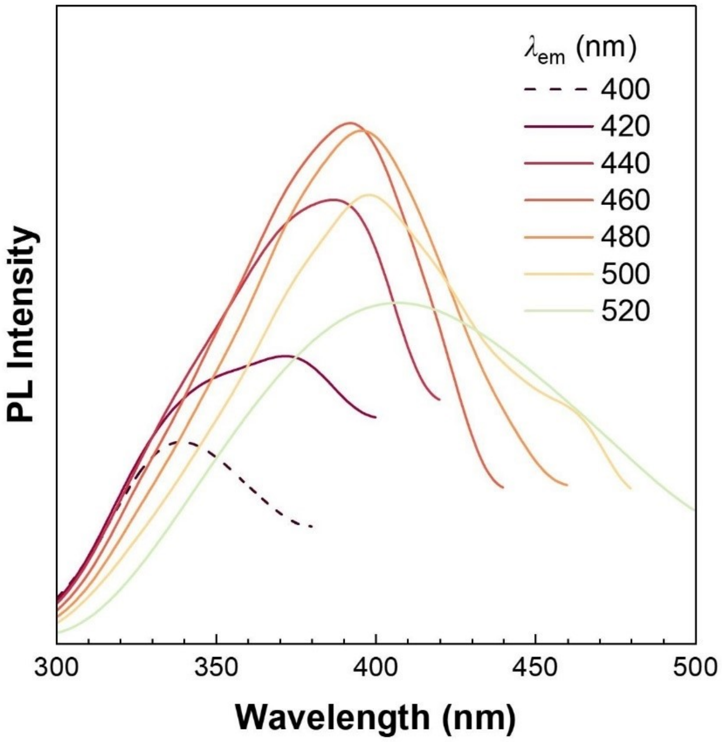

Figure S46. EX spectra of **P2** catalyzed by TEA/TEB in DCM (c = 10^{-1} M) with different λ_{em}.

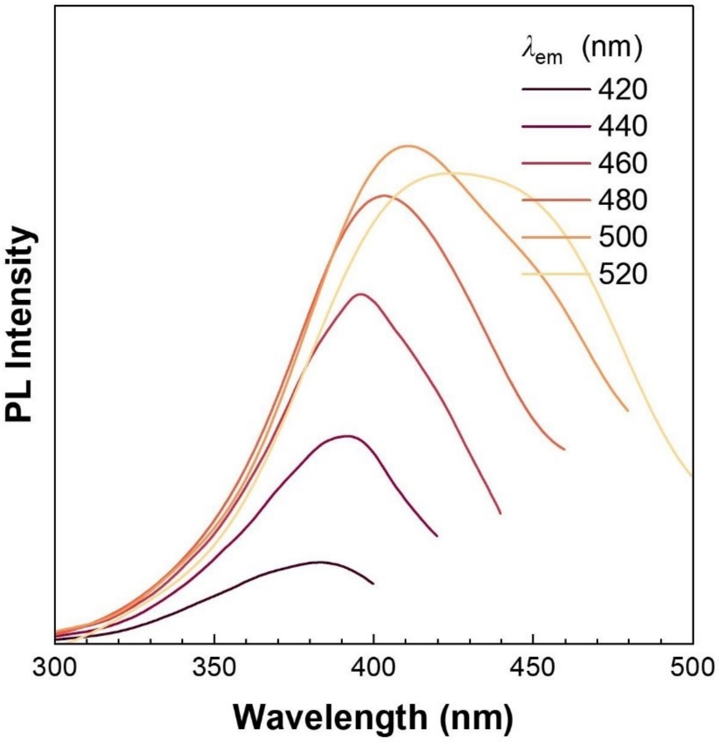

Figure S47. EX spectra of **P3** catalyzed by TEA/TEB in DCM (*c* = 10^{-1} M) with different λ_{em}.

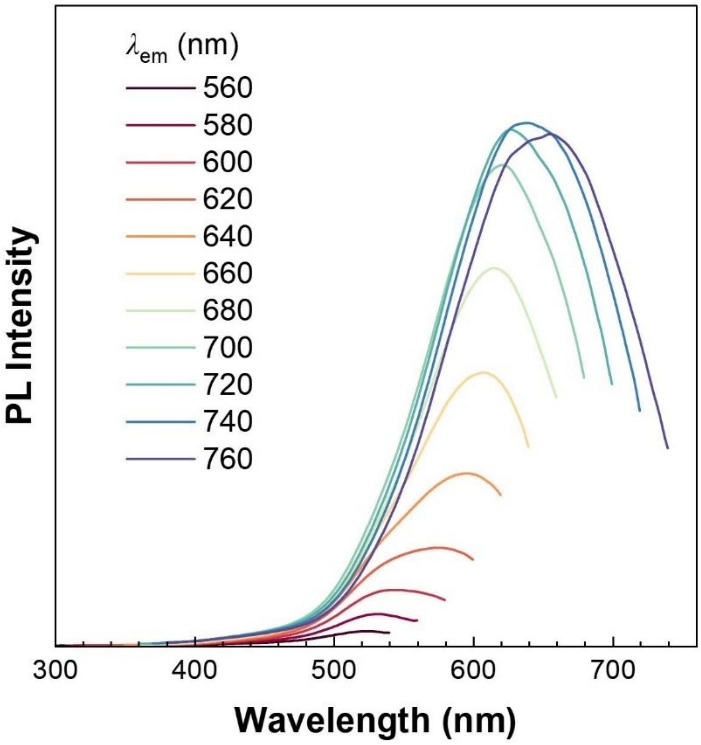

Figure S48. EX spectra of **P4** catalyzed by TEA/TEB in DCM (*c* = 10^{-1} M) with different λ_{em}.

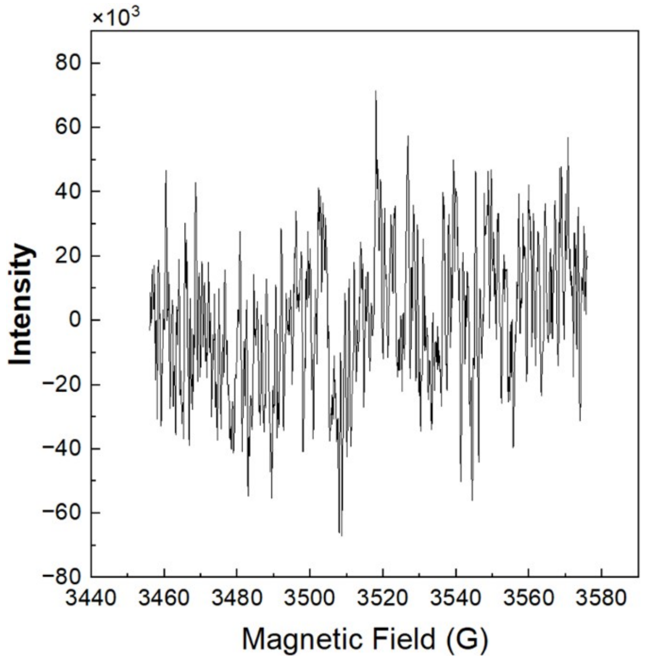

Figure S49. EPR spectrum of **P4** in DCM (20 mg/ml).

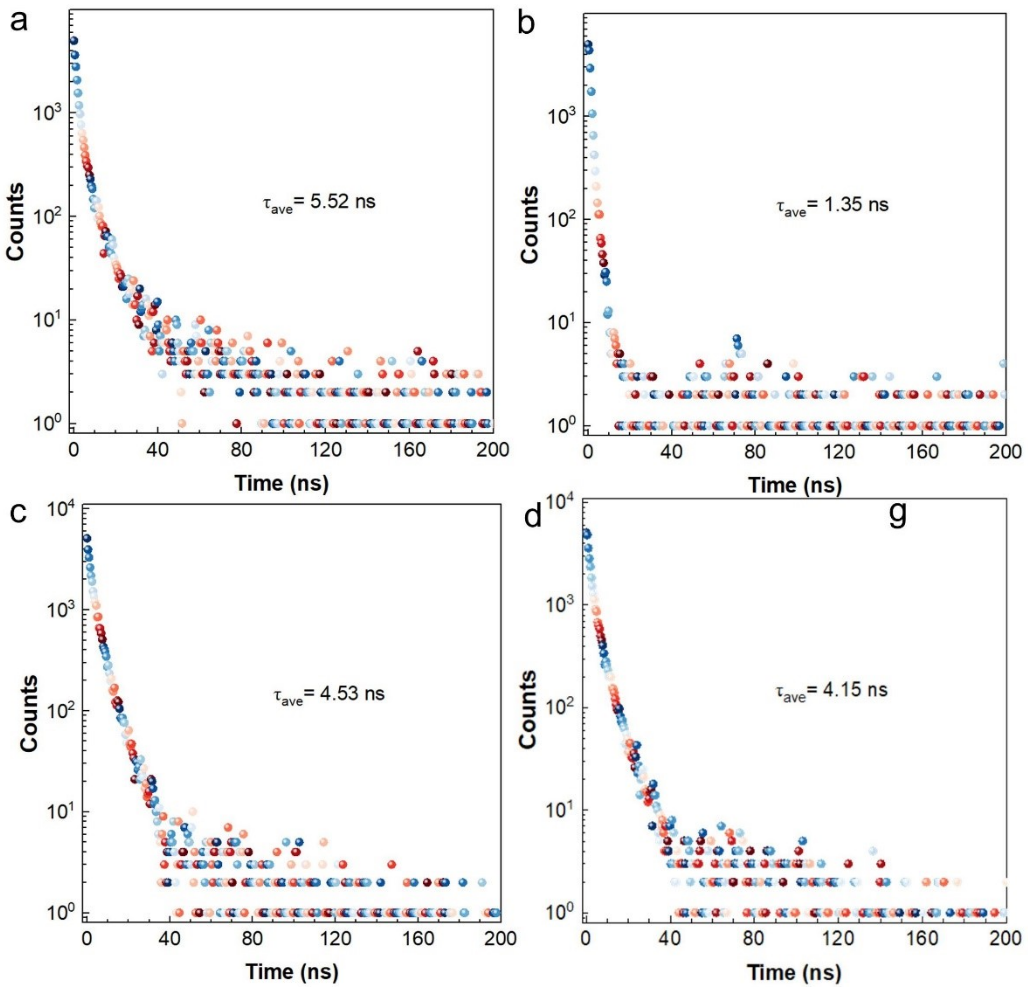

Figure S50. Time-resolved PL decay curves of polyesters a) **P1**, λ_{ex} = 360 nm, λ_{em} = 468 nm; b) **P2**, λ_{ex} = 405 nm, λ_{em} = 474 nm; c) **P3**, λ_{ex} = 405 nm, λ_{em} = 518 nm and d) **P4**, λ_{ex} = 470 nm, λ_{em} = 680 nm in solid state.

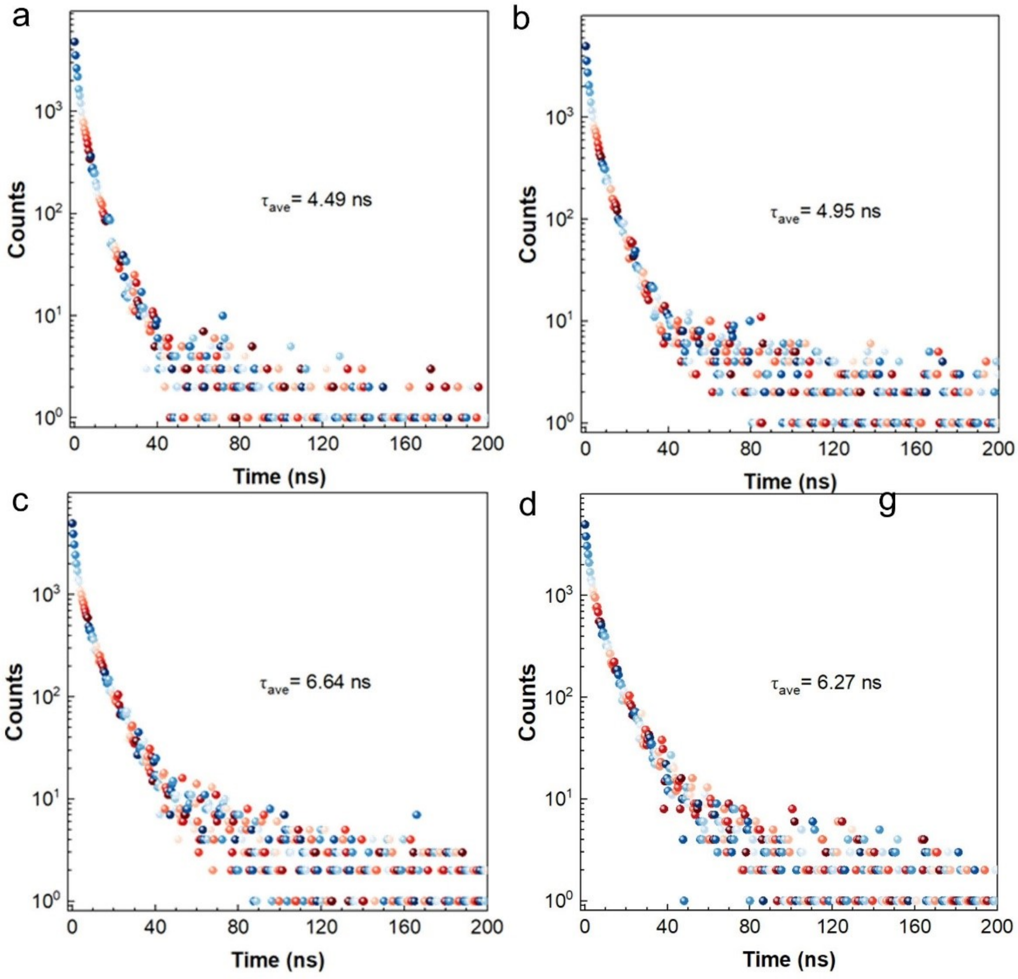

Figure S51. Time-resolved PL decay curves of polyesters a) **P1**, λ_{ex} = 360 nm, λ_{em} = 430 nm; b) **P2**, λ_{ex} = 405 nm, λ_{em} = 470 nm; c) **P3**, λ_{ex} = 405 nm, λ_{em} = 470 nm and d) **P4**, λ_{ex} = 470 nm, λ_{em} = 640 nm in DCM (10^{-2} M).

Table S1. Summary of physical properties of P1~P4.

Sample	M_n[a] (kg/mol)	PDI[a]	λ_{abs}[b] (DCM)(nm)	λ_{em}[c] (DCM)(nm)	λ_{em}[d] (solid)(nm)	Φ[c] (DCM, %)	Φ[d] (solid, %)	τ[e] *(ns)*	τ[d] *(ns)*
P1	17.3	1.49	225, 280	430	468	4.6	16.1	4.49	4.53
P2	8.7	1.57	227, 300	480	474	5.7	7.7	4.95	5.58
P3	1.5	2.03	224, 330	510	518	3.8	5.0	6.64	5.35
P4	3.9	1.70	237, 467	740	680	0.1	2.0	6.27	6.30

a: number-average molecular weight and polydispersity measured by GPC using THF as the eluent. b: UV-Vis absorption spectra in DCM (10^{-2} M). c: PL spectra and QY (for **P1**: λ_{ex} = 360 nm; for **P2**: λ_{ex} = 400 nm; for **P3**: λ_{ex} = 420 nm; for **P4**: λ_{ex} = 640 nm) in DCM (10^{-1} M); d: PL spectra, Time-resolved and PL decay curves QY (for **P1**: λ_{ex} = 380 nm; for **P2**: λ_{ex} = 420 nm; for **P3**: λ_{ex} = 440 nm; for **P4**: λ_{ex} = 480 nm) in solid. e: Time-resolved and PL decay curves in DCM (10^{-2} M).

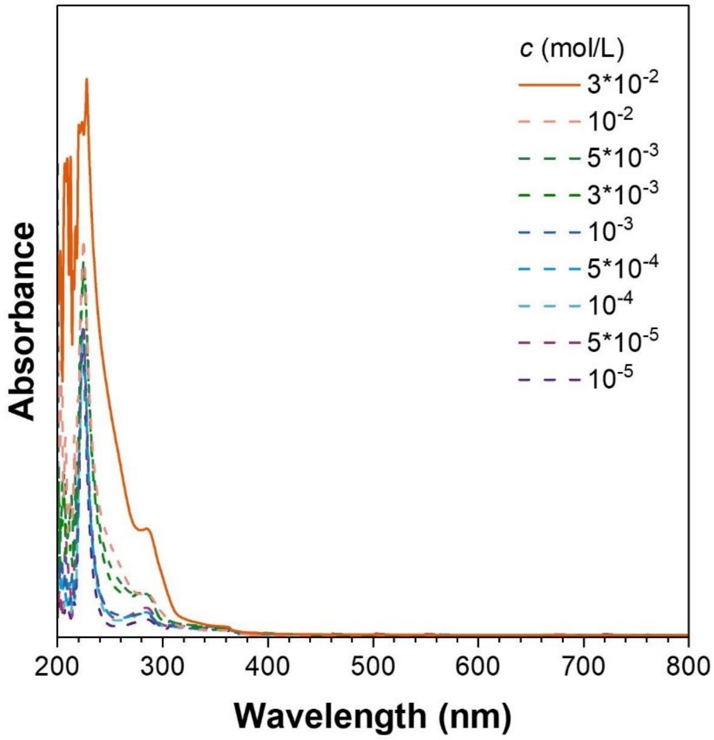

Figure S52. Concentration-dependent UV-Vis absorption spectra of **P1** in DCM (10^{-5} to $3*10^{-2}$ M).

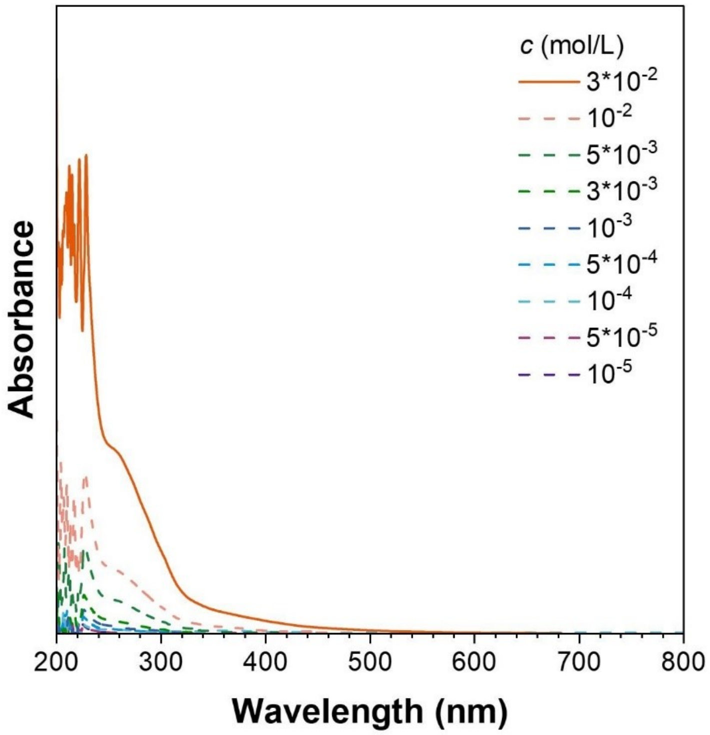

Figure S53. Concentration-dependent UV-Vis absorption spectra of **P2** in DCM (10^{-5} to $3*10^{-2}$ M).

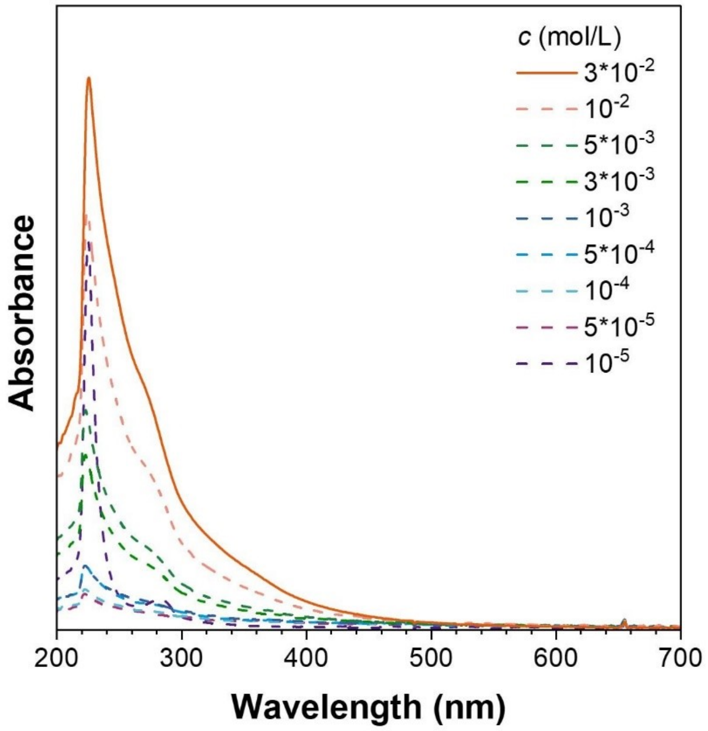

Figure S54. Concentration-dependent UV-Vis absorption spectra of **P3** in DCM (10^{-5} to $3*10^{-2}$ M).

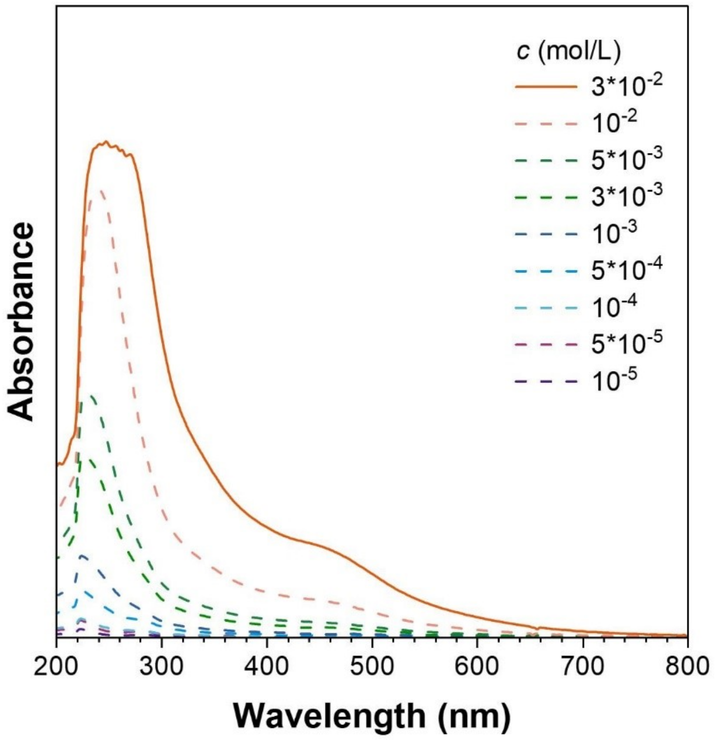

Figure S55. Concentration-dependent UV-Vis absorption spectra of **P4** in DCM (10^{-5} to $3*10^{-2}$ M).

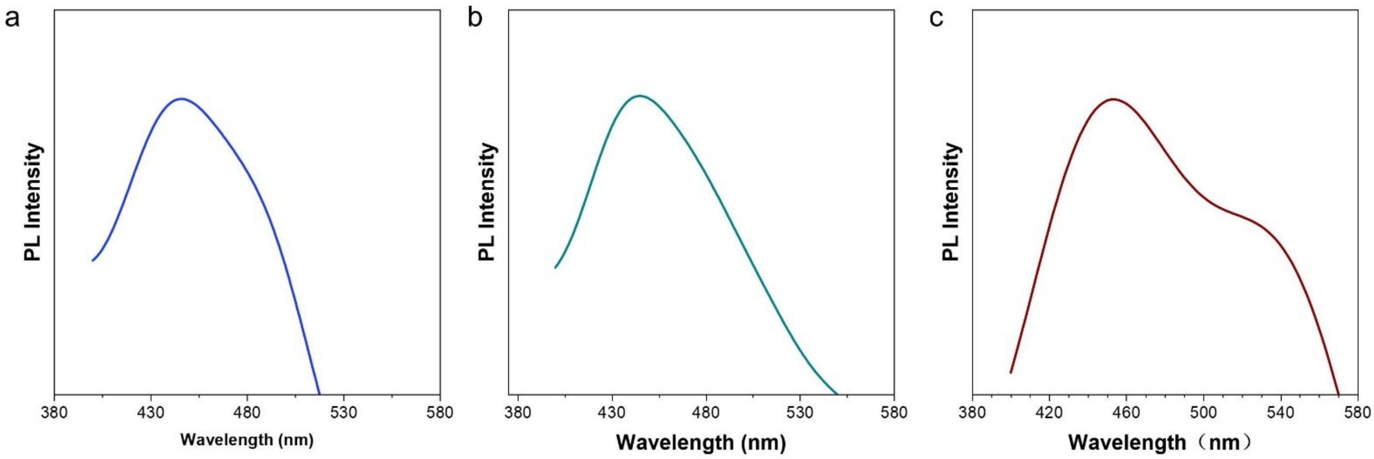

Figure S56. PL spectra of a) **P2,** b) **P3**, and c) **P4** in DCM (c =10^{-5} M, λ_{ex} = 380 nm), respectively.

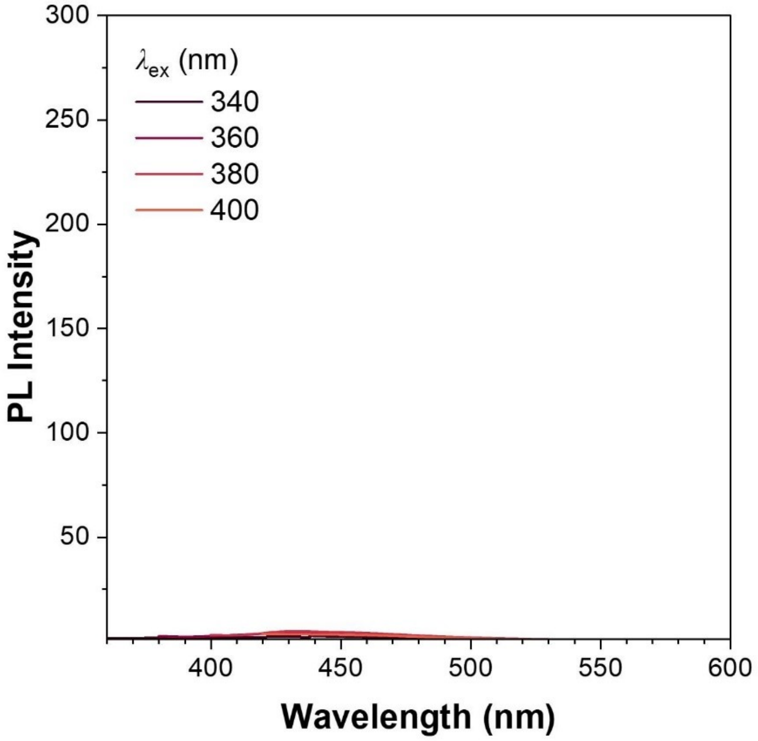

Figure S57. PL spectra of M1 with different λ_{ex}.

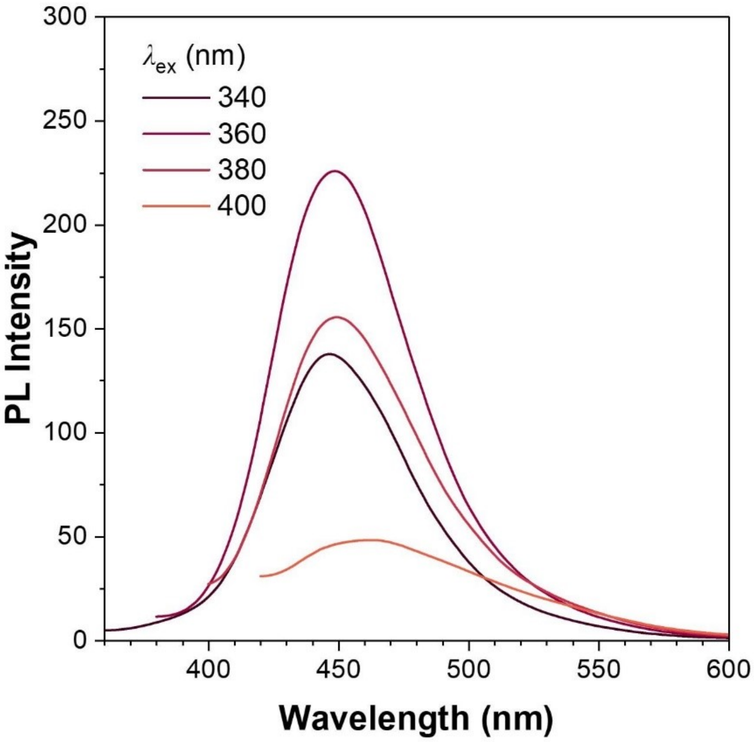

Figure S58. PL spectra of M4 with different λ_{ex}.

References

1. W. Humphrey, A. Dalke, K. Schulten, VMD: Visual Molecular Dynamics. *J. Mol. Graph.* **1996**, 14, 33-38.
2. Z. Liu, T. Lu, Q. Chen. An sp-hybridized all-carboatomic ring, cyclo[18]carbon: Electronic structure, electronic spectrum, and optical nonlinearity, *Carbon*. **2020**, 165, 461-467.
3. T. Lu, Chen, F. Multiwfn: a Multifunctional Wavefunction Analyzer. *J. Comput. Chem.* **2012**, 33, 580-592.